AD-A081 238 ITT ELECTRO-OPTICAL PRODUCTS DIV ROANOKE VA F/G 20/6
STUDY OF DYNAMIC EFFECTS ON GLASS FIBERS.(U)
NOV 79 F I AKERS, S L MAHURIN, G C SALISBURY N00014-78-C-0880
UNCLASSIFIED ITT-79-37-11 NL

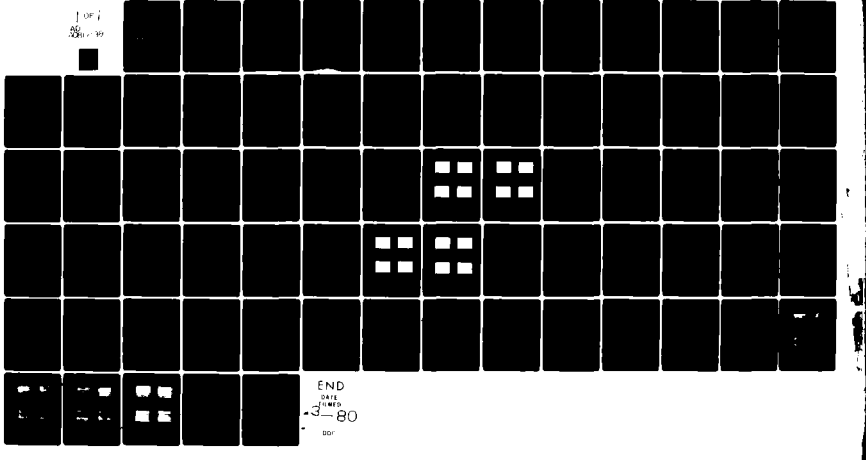

END
DATE FILMED
3-80
DDC

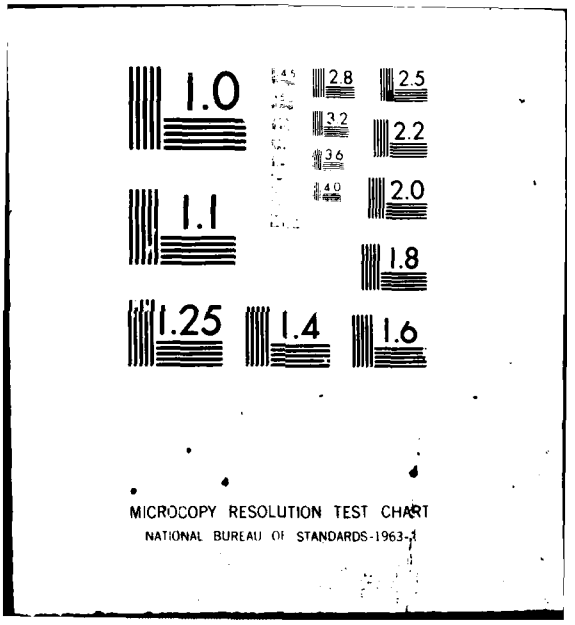
1.0
2.8
2.5
3.2
2.2
3.6
4.0
2.0
1.1
1.8
1.25
1.4
1.6
MICROCOPY RESOLUTION TEST CHART
NATIONAL BUREAU OF STANDARDS-1963-A

AD A081238

DTIC FILE COPY

FINAL TECHNICAL REPORT

STUDY OF DYNAMIC EFFECTS ON GLASS FIBERS

DTIC
FEB 27 1980
D
C

1 OCTOBER 1978 TO 30 NOVEMBER 1979

CONTRACT NO. N00014-78-C-0880

LEVEL II

PREPARED BY:

ITT *Electro-Optical Products Division*
7635 Plantation Road, Roanoke, Va. 24019

PREPARED FOR :

OFFICE OF NAVAL RESEARCH
800 N. QUINICY ST.
ARLINGTON, VIRGINIA 22217

79 12 5 001

ITT *Electro-Optical Products Division*

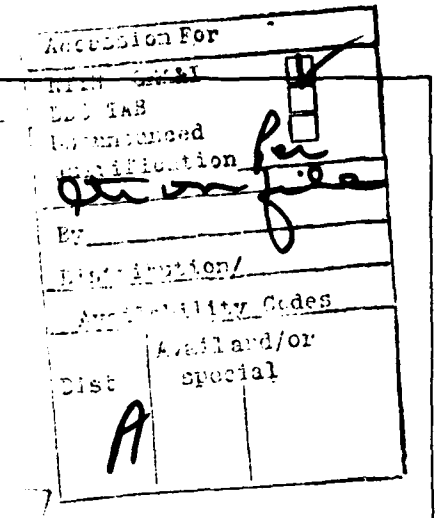

(6) STUDY OF DYNAMIC EFFECTS ON GLASS FIBERS,

(9) FINAL REPORT,

1 Oct [redacted] 78 - 30 Nov [redacted] 79

Contract Number: (15) N00014-78-C-0880

Prepared By

(10) F. I. Akers,
S. L. Mahurin
G. C. Salisbury

ITT Electro-Optical Products Division
P. O. Box 7065
Roanoke, Virginia 24019

For

Office of Naval Research
800 North Quincy Street
Arlington, Virginia 22217

Approved by:

R. E. Thompson, Manager of Fiber and Cable Research & Development

Approved by:

F. R. McDevitt, Director of Systems and Fiber Research and Development

(11) 26 Nov [redacted] 79

Roanoke, Virginia Doc Id No: 79-37-11

TABLE OF CONTENTS

PARAGRAPH	TITLE	PAGE
1.0	INTRODUCTION AND SUMMARY	1
2.0	SINGLE MODE FIBER DYNAMIC EFFECTS STUDY	4
2.1	Fiber Design	5
2.2	Fiber Fabrication Technique	7
2.2.1	Preform Fabrication	7
2.2.2	Fiber Drawing and Coating	8
2.3	Evaluation	13
2.3.1	Optical Evaluation	13
2.3.1.1	Mode Content	13
2.3.1.2	Attenuation	13
2.3.2	Dynamic Tension Test	14
2.3.3	Dynamic Twist Test	30
2.3.4	Dynamic Bend Tests	40
3.0	CONCLUSIONS AND RECOMMENDATIONS	66

LIST OF ILLUSTRATIONS

FIGURE	TITLE	PAGE
2.2.2-1	Optical Fiber Drawing Apparatus Diagram	10
2.3.2-1	Fiber Dynamic Tension Test Apparatus	16
2.3.2-2	Excess Loss Monitoring Equipment	18
2.3.2-3	Tension Test EMT-20721 Section 1	19
2.3.2-4	Tension Test EMT-20721 Section 2	20
2.3.2-5	Tension Test EMT-20793 Section 1	21
2.3.2-6	Tension Test EMT-20973 Section 2	22
2.3.2-7	Tension Test EM-20495 Section 1	23
2.3.2-8	Tension Test EM-20495 Section 2	24
2.3.2-9	Tension Test EMH-20726c Section 1	25
2.3.2-10	Tension Test EMH-20726c Section 2	26
2.3.2-11	Tension Test at 5 Hz	28
2.3.2-12	Tension Test at 10 Hz	29
2.3.3-1	Dynamic Twist Test Apparatus	31
2.3.3-2	Twist Test EMT-20721 Section 1	32
2.3.3-3	Twist Test EMT-20721 Section 2	33
2.3.3-4	Twist Test EMT-20793 Section 1	34
2.3.3-5	Twist Test EMT-20795 Section 2	35
2.3.3-6	Twist Test EM-20495 Section 1	36
2.3.3-7	Twist Test EM-20495 Section 2	37
2.3.3-8	Twist Test EMH-20726c Section 1	38
2.3.3-9	Twist Test EMH-20726c Section 2	39
2.3.3-10	Twist Test at 5 Hz	41
2.3.3-11	Twist Test at 10 Hz	42
2.3.4-1	Dynamic Bend Test Apparatus	43
2.3.4-2.1	Bend Test 6.4 mm Mandrel EMT-20721 Section 1	44
2.3.4-2.2	Bend Test 12.7 mm Mandrel EMT-20721 Section 1	45
2.3.4-3.1	Bend Test 6.4 mm Mandrel EMT-20721 Section 2	46
2.3.4-3.2	Bend Test 12.7 mm Mandrel EMT-20721 Section 2	47
2.3.4-4.1	Bend Test 6.4 mm Mandrel EMT-20793 Section 1	48
2.3.4-4.2	Bend Test 12.7 mm Mandrel EMT-20793 Section 1	49
2.3.4-5.1	Bend Test 6.4 mm Mandrel EMT-20793 Section 2	50
2.3.4-5.2	Bend Test 12.7 mm Mandrel EMT-20793 Section 2	51
2.3.4-6.1	Bend Test 6.4 mm Mandrel EM-20495 Section 1	52
2.3.4-6.2	Bend Test 12.7 mm Mandrel EM-20495 Section 1	53
2.3.4-7.2	Bend Test 12.7 mm Mandrel EM-20495 Section 2	54
2.3.4-7.1	Bend Test 6.4 mm Mandrel EM-20495 Section 2	55
2.3.4-8.1	Bend Test 6.4 mm Mandrel EMH-20726c Section 1	56
2.3.4-8.2	Bend Test 12.7 mm Mandrel EMH-20726c Section 1	57
2.3.4-9.1	Bend Test 6.4 mm Mandrel EMH-20726c Section 2	58
2.3.4-9.2	Bend Test 12.7 mm Mandrel EMH-20726c Section 2	59
2.3.4-10	Sample Dynamic Bend Test Strip Chart	60

LIST OF ILLUSTRATIONS (continued)

FIGURE	TITLE	PAGE
2.3.4-11	12.7 mm Mandrel Bend Test at 5 Hz	62
2.3.4-12	12.7 mm Mandrel Bend Test at 10 Hz	63
2.3.4-13	6.4 mm Mandrel Bend Test at 5 Hz	64
2.3.4-14	6.4 mm Mandrel Bend Test at 10 Hz	65

LIST OF TABLES

TABLE	TITLE	PAGE
2.2.1-1	Single Mode Fiber Fabrication Data	9
2.2.2-1	Properties of Special Coating Materials	12
2.3.1-1	Single Mode Fiber Optical Properties	15

1.0 INTRODUCTION AND SUMMARY

Single mode fibers are being employed as sensing elements in acoustic, rotation, and temperature sensors which are based upon optical phase change detection. Compact sensor designs require the fibers to be wound onto small diameter mandrels. In addition, deployment of these sensors will subject the single mode fibers to dynamic environmental stresses of a mechanical nature. These stresses include dynamic tension, twist, and bend.

Although 0.1 NA single mode fibers exhibit attenuation less than 3 dB/km in an unstressed configuration, their loss increases to more than 40 dB/km when tightly coiled. Static bending losses in single mode fibers were eliminated by the development of a 0.2 NA fiber under NRL contract N00173-78-C-0196. In order to predict the impact of environmental mechanical stresses on fibers used in sensor applications, ITT EOPD was awarded contract N00014-78-C-0880 by the Office of Naval Research for the study of the effects of dynamic tension, twist, and bend on the optical properties of both 0.1 and 0.2 NA single mode fibers.

In accordance with the statement of work of Contract N00014-78-C-0880, EOPD has evaluated the effects of dynamic tension, twist,

and bend on single mode fibers. This program had the following objectives:

a. Fabrication of single mode fibers having NA values of 0.1 and 0.2, using a borosilicate cladding and a germanosilicate core

b. Coating of the fibers with two coating systems. These include standard silicone RTV primary coating and polyester secondary jacket, in addition to coating of the fiber with a material having a refractive index equal to or greater than the fused quartz substrate tube

c. Evaluation of the attenuation of the above fibers in an unstressed condition and while subjecting them to dynamic bend, twist, and tension

All of the above objectives were met. Single mode fibers were fabricated using borosilicate cladding and germanosilicate core. These fibers had NA values of 0.11 and 0.21, and were coated with silicone primary and polyester secondary jacket materials. In addition, a 0.11 NA fiber was coated with a thermally cured Dow-Corning conformal coating having a 1.48 refractive index, and a 0.19 NA fiber was coated with an ultra-vilot cured coating having a refractive index of 1.52. In addition to static attenuation evaluation of all fibers at three wavelengths, the attenuation of all fibers was measured at 0.63 μm while they were subjected to dynamic tension, twist, and bend at three frequencies.

The dynamic tension and twist had minimal effect on fiber attenuation. The low NA fiber was substantially affected by

dynamic bending, while the high NA fiber was not affected by the extreme bend over a 6.3 mm diameter mandrel. No effects due to dynamic interactions were found, since fiber attenuation effects could be explained in terms of static twisting, tension, and bending. In addition, the jacket refractive index had no detectable effect on dynamic behavior.

Section 2 discusses, in detail, the results of the single mode fiber dynamic effects study.

2.0 SINGLE MODE FIBER DYNAMIC EFFECTS STUDY

ITT EOPD is currently producing 0.11 NA single mode fibers having V_c = 2.2 at 0.63 μm. These fibers are being purchased primarily for fiber gyro and acoustic sensor applications. Attenuation values as low as 2 dB/km at 0.85 μm have been achieved for this fiber when evaluated in an unstressed configuration, and a value of 3.8 dB/km has been measured in a 1200 m long T-110 fiber which was level wound onto a 30 cm diameter spool. However, the optical loss increases to more than 40 dB/km when the T-110 fiber is spooled onto a 10 cm diameter spool.

As a result, EOPD recently developed a 0.2 NA single mode fiber under NRL Contract N00173-78-C-0196. This fiber was developed using three different core compositions of SiO_2/GeO_2, SiO_2/P_2O_5, and $SiO_2/GeO_2/P_2O_5$. The 0.2 NA fiber has a 2.2 μm core diameter and was evaluated for attenuation in two configurations: unstressed while strung between two 30 cm diameter drums and spooled onto a standard 10 cm diameter fiber spool. The 0.2 NA fiber had no measurable loss increase with respect to the strung configuration when wound onto the 10 cm diameter spool.

In order to evaluate the effects of dynamic tension, twist and bend on single mode fiber attenuation, preforms and fibers were

fabricated having 0.1 and 0.2 NA using borosilicate cladding and germanosilicate core materials. These fibers were coated with a standard silicone and polyester jacket combination. In addition, in order to evaluate the effects of high refractive index coating materials on fiber attenuation, both low and high NA single mode fibers were coated with experimental materials having refractive indices greater than the silica substrate index of 1.46.

Special test equipment and procedures were developed for valid evaluation of dynamic tension, twist, and bend effects on fiber loss. The remainder of this section describes the design, fabrication, and dynamic evaluation of low and high NA single mode fibers.

2.1 Fiber Design

In a single mode fiber, the normalized core diameter V_c must be small so that only the fundamental HE_{11} mode will propagate. This condition is satisfied when $V_c < 2.405$, which is the cut-off value V_{co} for the LP_{11} second order mode. The normalized core diameter is related to the fiber core diameter (dc), numerical aperture (NA), and operating wavelength (λ) through the equation:

$$V_c = \frac{dc\ \pi\ NA}{\lambda} \qquad (1)$$

The HE_{11} mode has no cut off, but as V_c becomes smaller, the normalized mode diameter increases such that the mode becomes weakly guided and becomes susceptible to bending and microbending losses.

Although the least bend-sensitive fiber would have a V_c value approaching 2.405, a smaller V_c design value must be used since practical uncertainties in measurement of preform cane NA and preform core diameter, and variations in fiber diameter during drawing cause an uncertainty in the actual fiber V_c value which can result in multimode operation. Fibers for this study were designed having $V_c = 0.9\ V_{co} = 2.2$ at 0.63 μm wavelength. Thus, selection of nominal fiber NA values of 0.1 and 0.2 fixed the core diameters at 4.4 μm and 2.2 μm respectively, according to equation 1.

The fiber NA results from reducing the cladding refractive index or raising the core refractive index or both. Typically, B_2O_3 is added as a dopant to SiO_2 to reduce the cladding index, while the core index is increased by the addition of GeO_2 or P_2O_5 to the base SiO_2 glass. Since an increase in core dopant level usually leads to an increase in Rayleigh and non-Rayleigh scattering losses of the core glass, a design goal was to minimize core dopant concentration. As a result, the

metered dopant level in the 0.1 NA fiber was <5% GeO_2 by weight with a 5% B_2O_3 cladding dopant level. In the high NA fibers, the cladding refractive index was depressed to near its minimum value reported at 15% B_2O_3. Furthermore, the core dopant level was adjusted to achieve the desired NA. Because an appreciable portion of the light power propagates in the cladding portion of a single mode fiber, the cladding thickness was designed to be at least eight times the core radius. This insured that most of the field is contained within the high purity deposited cladding material and that inward diffusion of impurities from the starting substrate has a minimal effect on optical transmission.

2.2 Fiber Fabrication Technique

Single mode fibers are produced by fabricating an 8 mm diameter preform rod, then drawing the preform into a nominally 80 μm diameter fiber. Coatings are applied during the drawing operation. The following two sections describe these operations.

2.2.1 Preform Fabrication

Fiber preforms were fabricated by the modified chemical vapor deposition technique (MCVD) using mass flow control of chemical reactants. Bubble free high purity natural fused quartz tubing was used for the substrate material, into which

optical cladding and core materials were deposited. Table 2.2.1-1 summarizes the core and cladding compositions and the core and cladding passes used for the preforms. The low NA preforms required 10 passes of core in order to provide a fiber having a 4.4 μm core in about 80 μm od fiber. Fewer core passes were used for the high NA preform so that a 2.2 μm core would result in an 80 μm fiber. The cladding and core dopant concentrations were adjusted to produce the desired NA value. After the deposition was completed, the preform tube was heated intensely and collapsed to a solid rod. The preform was then drawn to the diameter necessary to yield fiber having V_c = 2.2 at 0.63 μm.

The preforms for specially coated fibers were modified to increase the preform and fiber diameters by collapsing one (EMT-20726C) or two (EMT-20793) additional substrate tubes over the finished preform.

2.2.2 Fiber Drawing and Coating

The preforms were drawn to fibers of the desired diameter with the equipment shown schematically in Figure 2.2.2-1. The preforms were drawn using a graphite resistance furnace. Furnace drawn fibers, in contrast to flame drawn fibers, exhibit better diameter uniformity but lower strength. The fiber

Table 2.2.1-1. Single Mode Fiber Fabrication Data.

Preform No.	Preform Diameter (mm)	NA (±0.01)	Core Passes	Clad Passes	WT % B_2O_3 In Clad	WT % Core Dopant
EMT-20721	8.3	0.11	10	50	4.8	4.3
EM-20495	9.0	0.21	3	50	13.7	36.1
EMT-20793	17.8	0.11	10	50	4.8	4.3
EMT-20726C	11.4	0.19	10	25	13.7	36.2

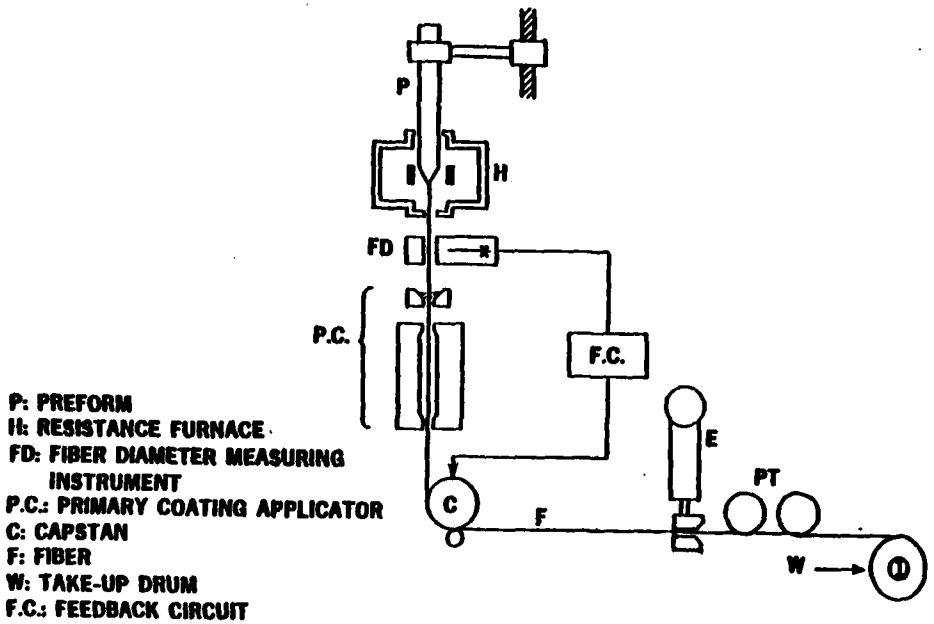

Figure 2.2.2-1. Optical Fiber Drawing Apparatus Diagram.

diameter was monitored continuously and was controlled within ±2%. Fibers were dip coated on-line with a primary coating of low modulus silicone resin Sylgard® 184, to a nominal diameter of 300 µm. The refractive index of Sylgard® 184 is 1.43. Also a secondary jacket of Hytrel® type 72D jacket was extruded on-line to a nominal final diameter of 400 µm. The fibers were collected on 10 cm diameter spools as they were drawn.

Two fibers were coated with materials which had refractive indices greater than the substrate glass index of 1.46. The properties of these special coating materials are listed in Table 2.2.2-1. The Dow-Corning conformal coating is a thermally curable silicone resin, whereas WCC-2® is an ultravilot curable resin. The Dow Corning coating had a very slow curing rate compared to the standard silicone material. Thus, it was necessary to modify the dip-coater design, so as to apply a coating thickness less than 26 µm. In addition, the temperature profile of the curing oven was adjusted to achieve a tack-free, smooth, uniform coating on the fiber. A secondary jacket of polyester was applied over the conformal coating. The WCC-2® was applied by dip-coating to a nominal thickness of 60 µm and was cured on line, using a UV lamp system. No secondary jacket was applied to this fiber.

Table 2.2.2-1. Properties of Special Coating Materials.

Material	Composition	Properties					
		Physical			Mechanical		
		Specific Cavity%25°C	RI @25°C	Viscosity @25°C (cps)	Durometer Hardness (points)	Tensile Strength (psi)	Elongation (%)
Dow-Corning conformal coating	Phenyl-methyl dimethyl silicone	1.07	1.48	800	45$^{\Delta}$	650	15
W.R. Grace WCC-2	Polyene/polythiol ester	1.20	1.52	4000	93*	2500	70

ΔShore D

*Shore A

2.3 Evaluation

The fibers produced in this program were evaluated to determine optical transmission properties in the unstressed state and attenuation effects when subjected to dynamic stress.

2.3.1 Optical Evaluation

The optical properties measured include fiber mode content at 6328Å and fiber attenuation at 0.63, 0.83, and 1.03 μm. These tests were performed to eliminate any multimode fibers from the test program and to establish base line fiber transmission data.

2.3.1.1 Mode Content

To determine whether a fiber propagates single or multiple modes at 6328Å, a five meter section is injected with radiation from a He-Ne laser. Both fiber ends are mode stripped to prevent power propagation in the substrate glass. The input spot is then radially scanned across the fiber end face while the operator views the far field output pattern. A multimode fiber will show variations in the nominal gaussian pattern. All multimode fibers are excluded from further testing.

2.3.1.2 Attenuation

The attenuation of single mode fibers is measured at wavelengths

of 0.63, 0.83, and 1.03 μm. The selection of multiple wavelengths provides additional fiber characterization data. Attenuation is evaluated by the injection loss technique, using optical filters with .01 micron bandwidth. All measurements are made with the fiber strung between two 30 cm diameter drums. The attenuation values measured for all single mode fibers produced for this contract are shown in Table 2.3.1-1.

2.3.2 Dynamic Tension Test

Among the environmental stresses which could act upon a deployed single mode fiber is dynamic tension. This stress is simulated by the equipment of Figure 2.3.2-1.

The test fiber is secured to the surface of the moving carriage with the carriage in its midpoint position. The fiber is also clamped at a point 127 cm (50 in) from the carriage contact. A nominal tension is maintained to remove any slack in the fiber. The motor drive provides a displacement of ±2.54 cm (±1.0 in) representing a fiber load of 1.37×10^9 N/m^2 (200 KPSI) at 2% elongation. Differential fiber attenuation is measured at translation frequencies of 0, 5, and 10 Hz.

Two adjacent sections of four different fiber types were tested. All tests utilized the tap-off monitoring coupler

Table 2.3.1-1. Single Mode Fiber Optical Properties.

Fiber No.	Coating	NA	Attenuation (±0.3 dB/km) .63 μm	.83 μm	1.03 μm
EMT-20721	Silicone/polyester	0.11	7.3	2.4	2.4
EM-20495	Silicone/polyester	0.21	20.2	8.7	5.0
EMT-20793	Conformal/polyester	0.11	34.4	21.9	NT
EMH-20726C	Polyene-polythiol Ester	0.19	50.4	25.0	NT

NT = No detectable transmission

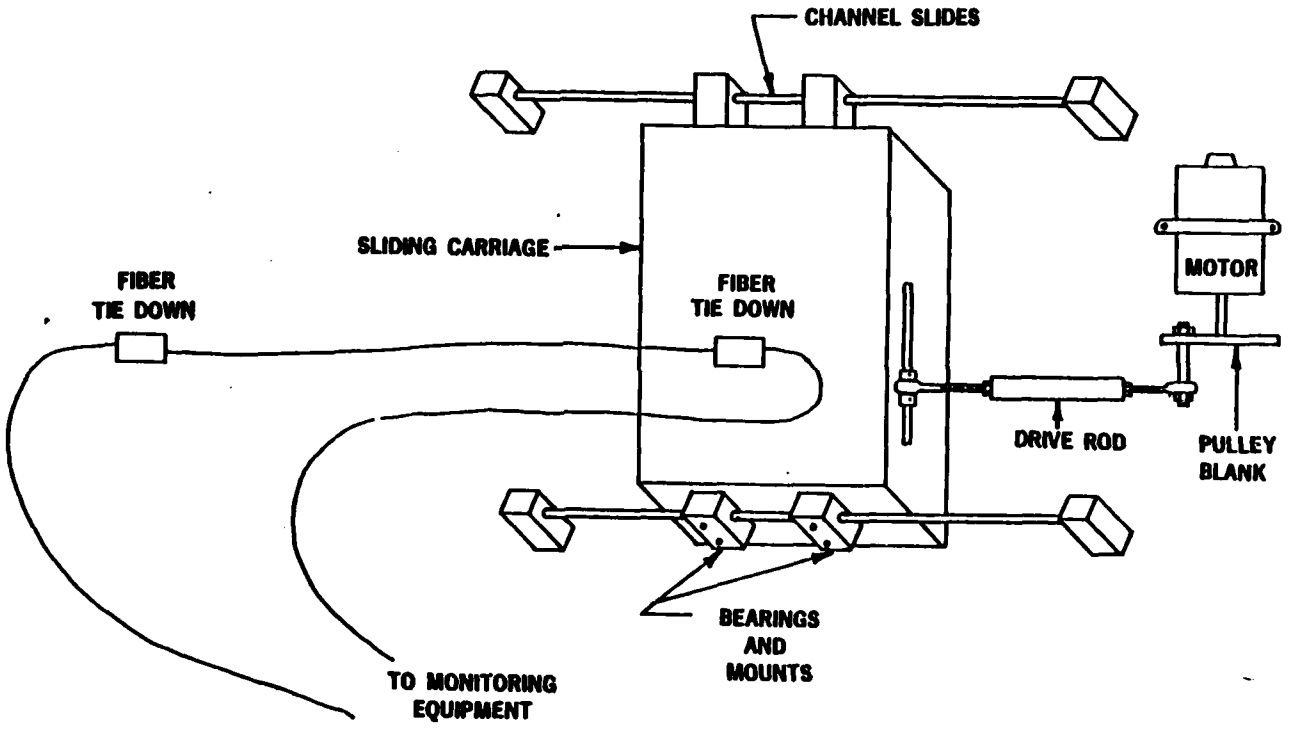

Figure 2.3.2-1. Fiber Dynamic Tension Test Apparatus.

described in the progress report previously submitted for contract N00014-78-C-0852, titled "Single Mode Fiber Bend Loss Study." This coupler enables the monitoring of the input power level during the test. This increases the accuracy of the attenuation measurements by isolating output power variations due to environmental stresses from input power variations.

Two sets of experiments were conducted. The first set utilized the monitoring equipment of Figure 2.3.2-2. Two lock-in amplifiers provide stable, low noise detection of both the coupler and output power levels. The output of both lock-in amplifiers is recorded by a dual pen strip chart recorder. The differential attenuation induced by the applied stress is determined by comparing the coupler and output levels under stress with the unstressed values. The relation used is:

$$\Delta\alpha_i = 10 \log \frac{V_{tap\ i}}{V_{out\ i}} - 10 \log \frac{V_{tap\ o}}{V_{out\ o}}$$

where "i" designated the measurement period of interest and "o" represents the original values.

The data obtained from the eight sections tested for dynamic tension effects are shown in Figures 2.3.2-3 through 2.3.2-10. As anticipated, very little effect on attenuation was observed.

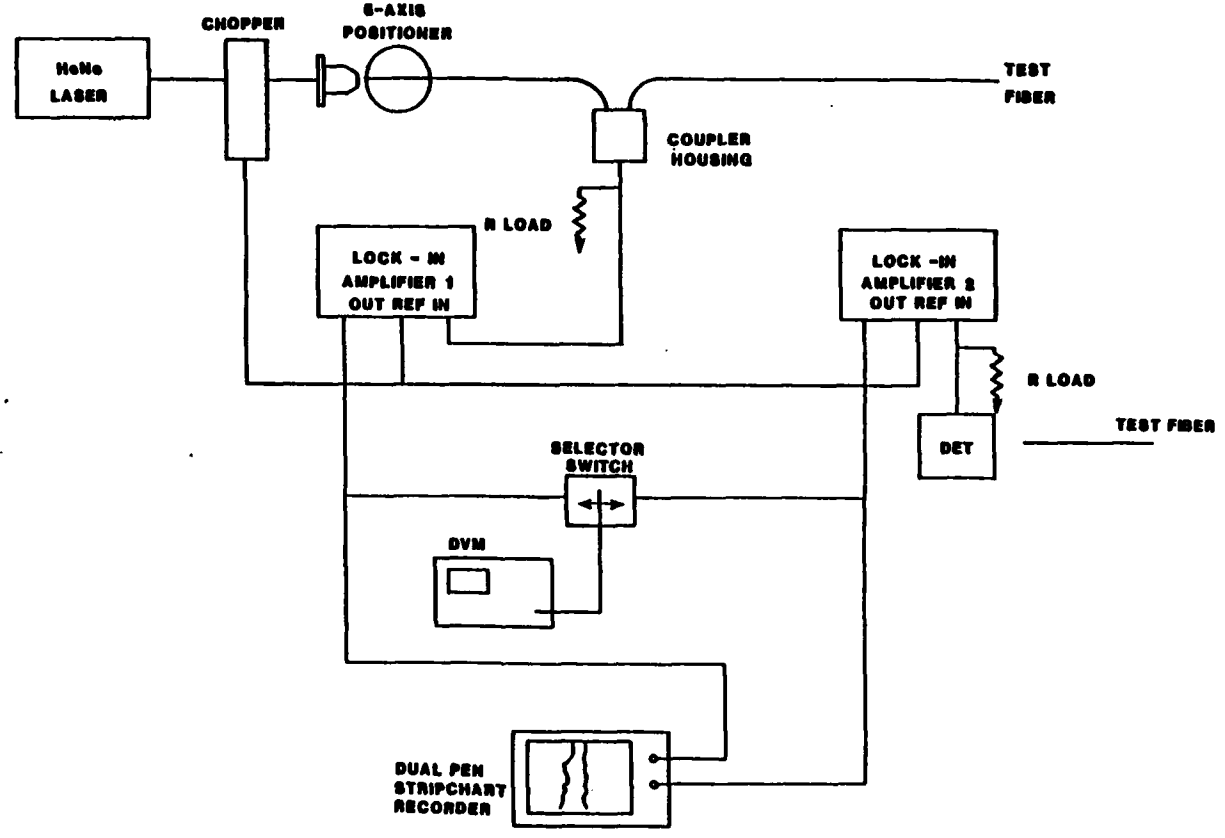

Figure 2.3.2-2. Excess Loss Monitoring Equipment.

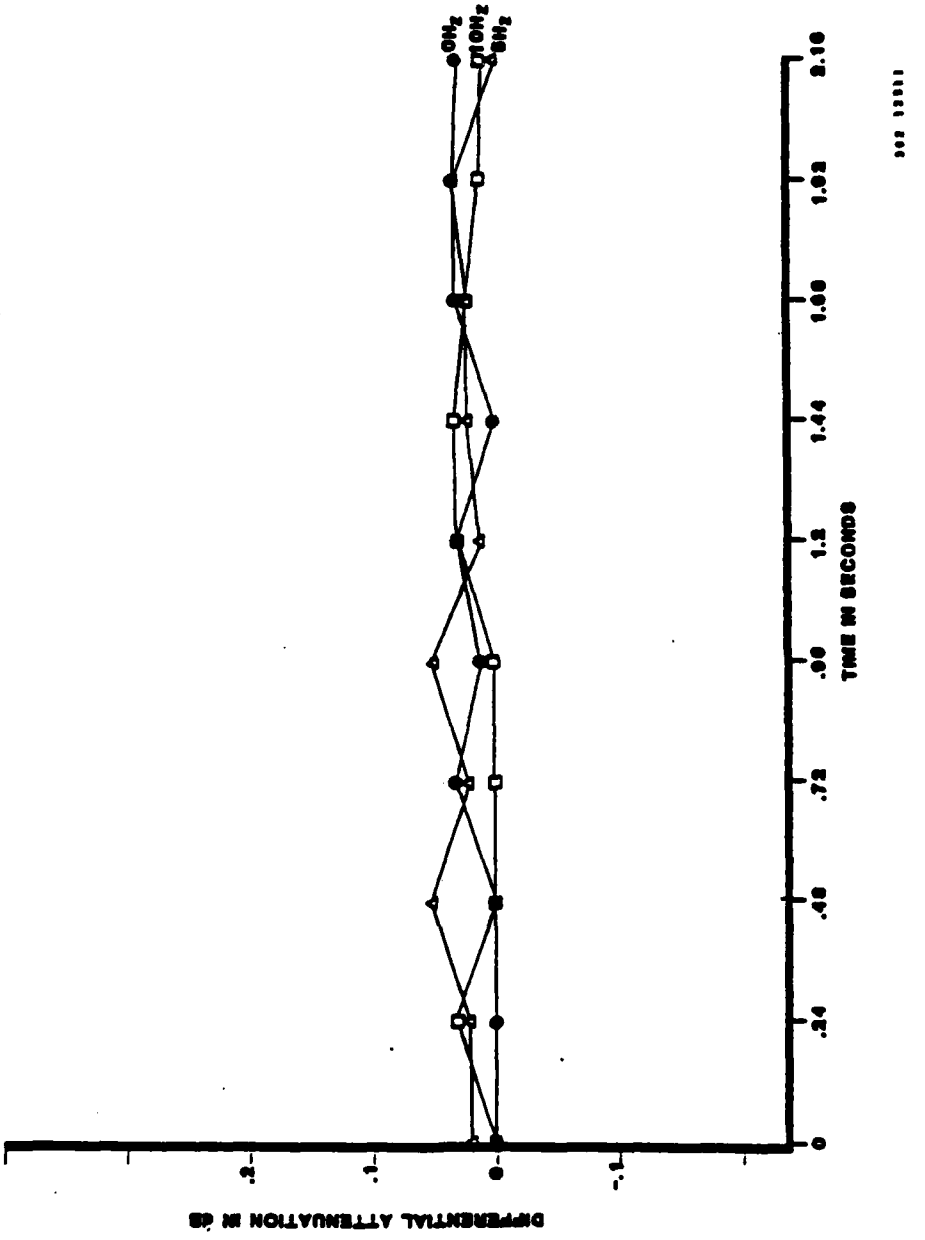

Figure 2.3.2-3. Tension Test EMT-20721 Section 1.

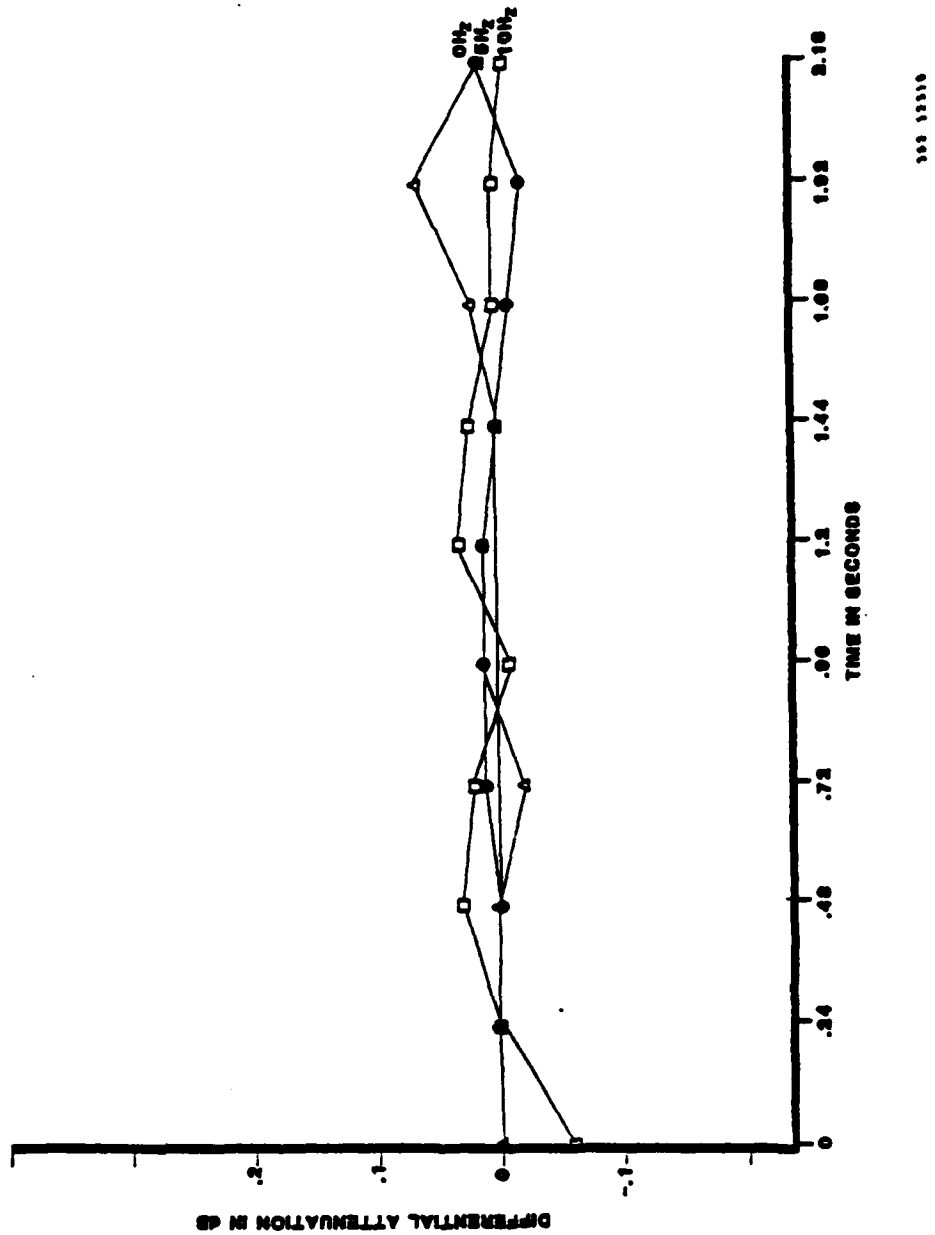

Figure 2.3.2-4. Tension Test EMT-20721 Section 2.

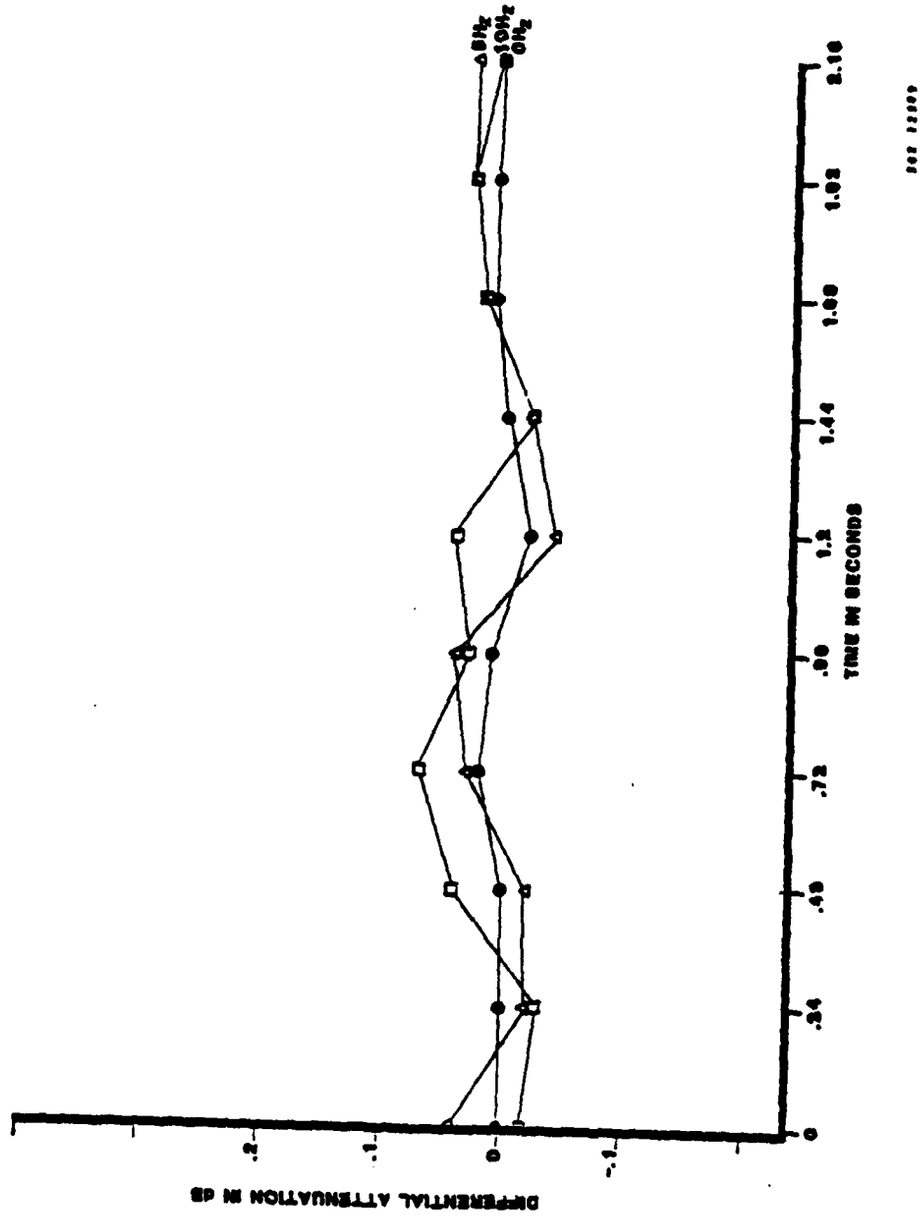

Figure 2.3.2-5. Tension Test EMT-20793 Section 1.

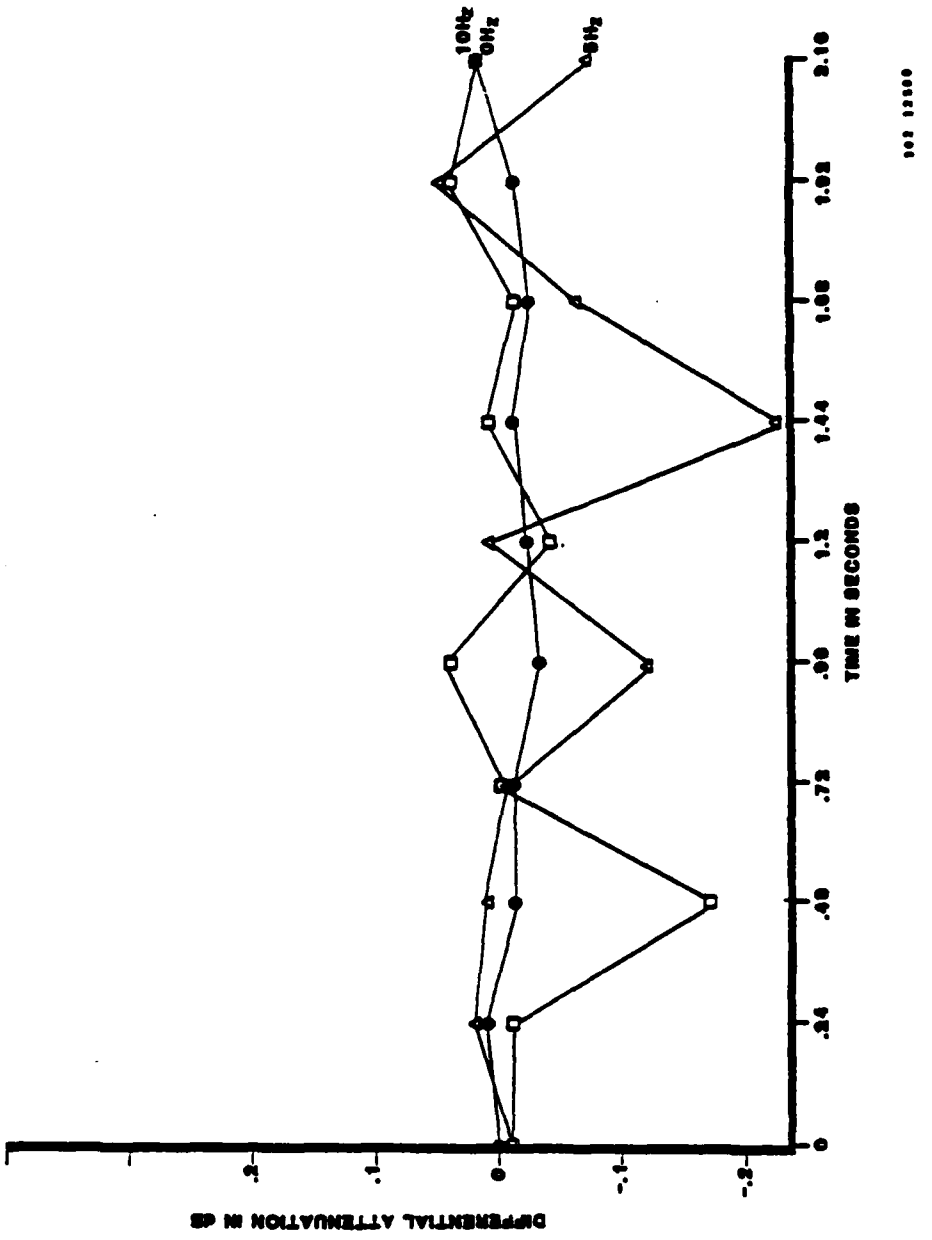

Figure 2.3.2-6. Tension Test EMT-20973 Section 2.

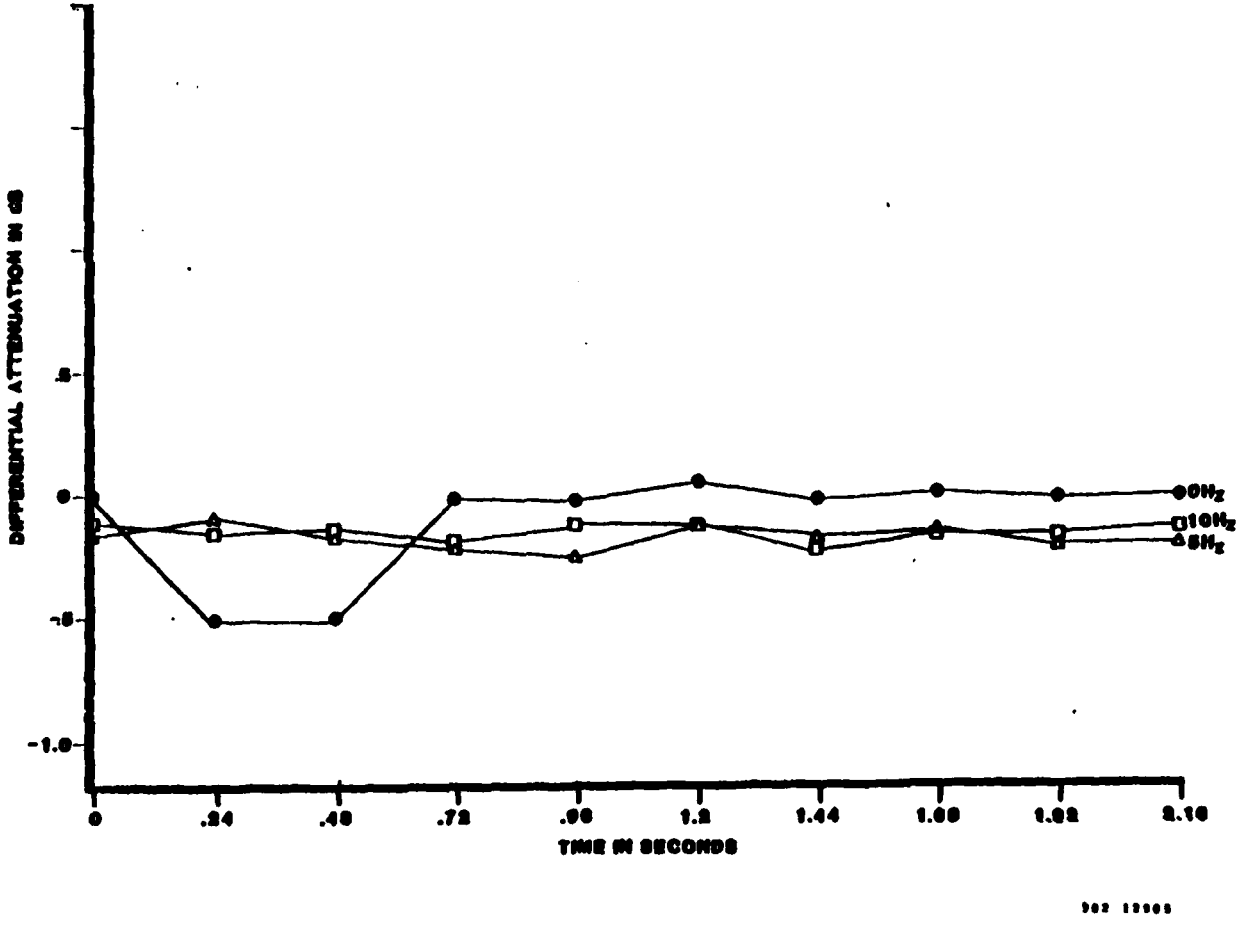

Figure 2.3.2-7. Tension Test EM-20495 Section 1.

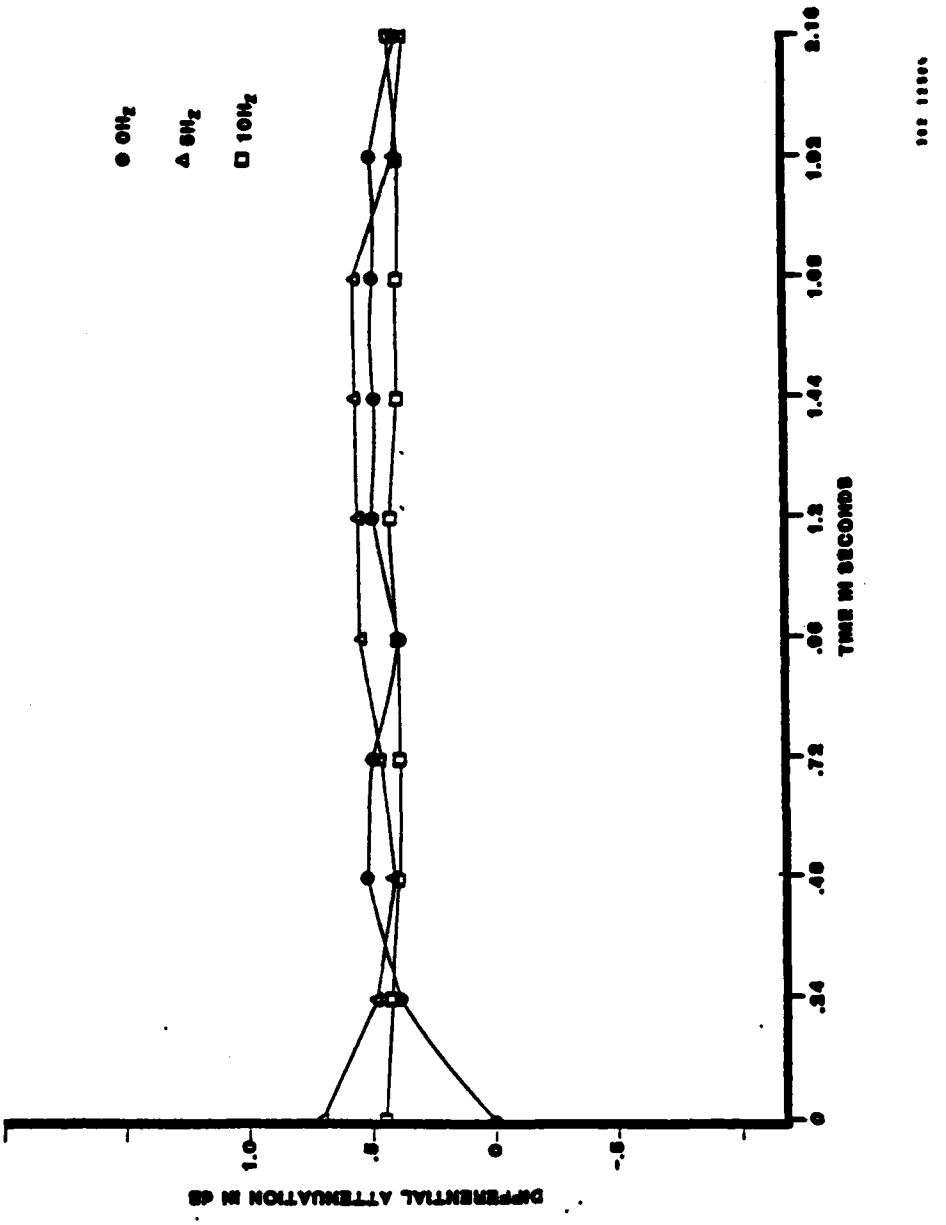

Figure 2.3.2-8. Tension Test EM-20495 Section 2.

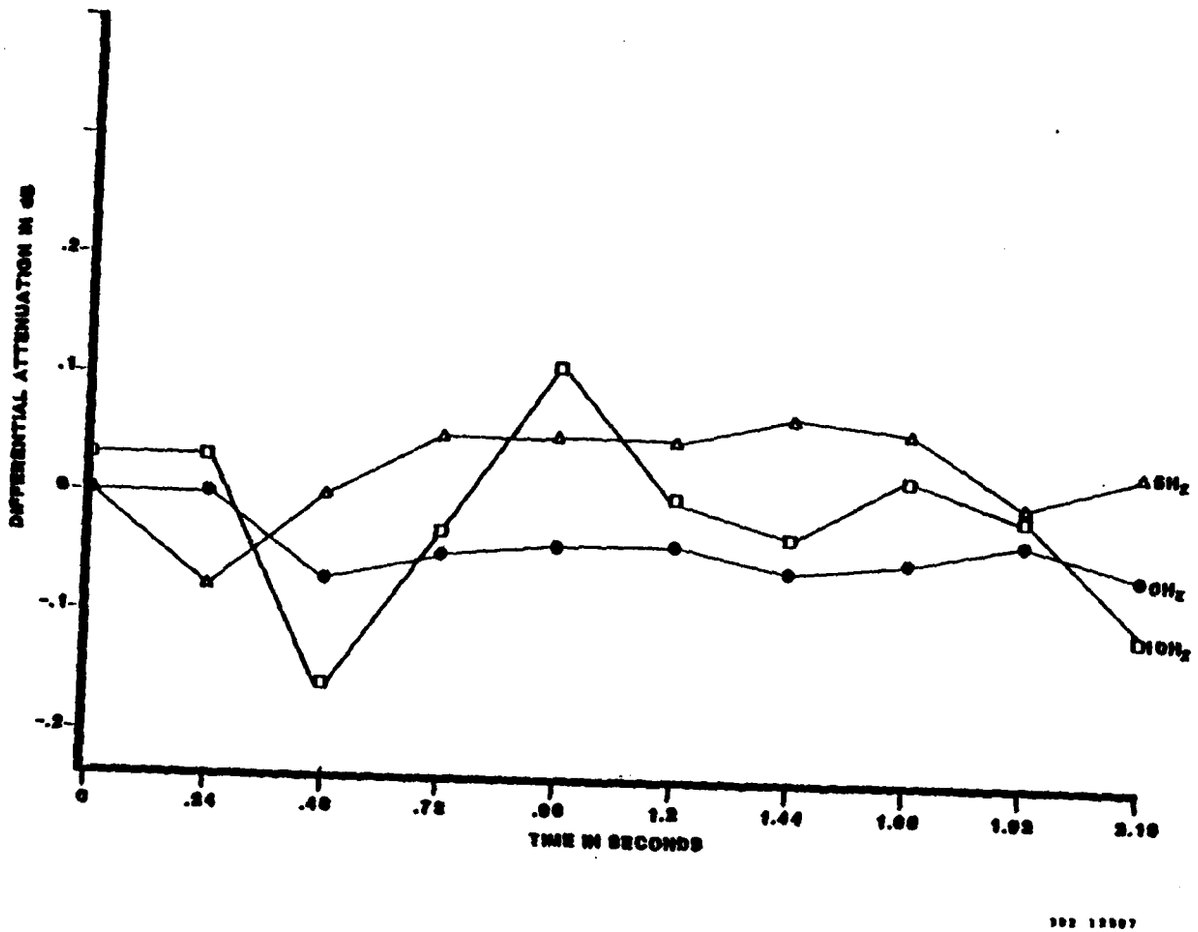

Figure 2.3.2-9. Tension Test EMH-20726c Section 1.

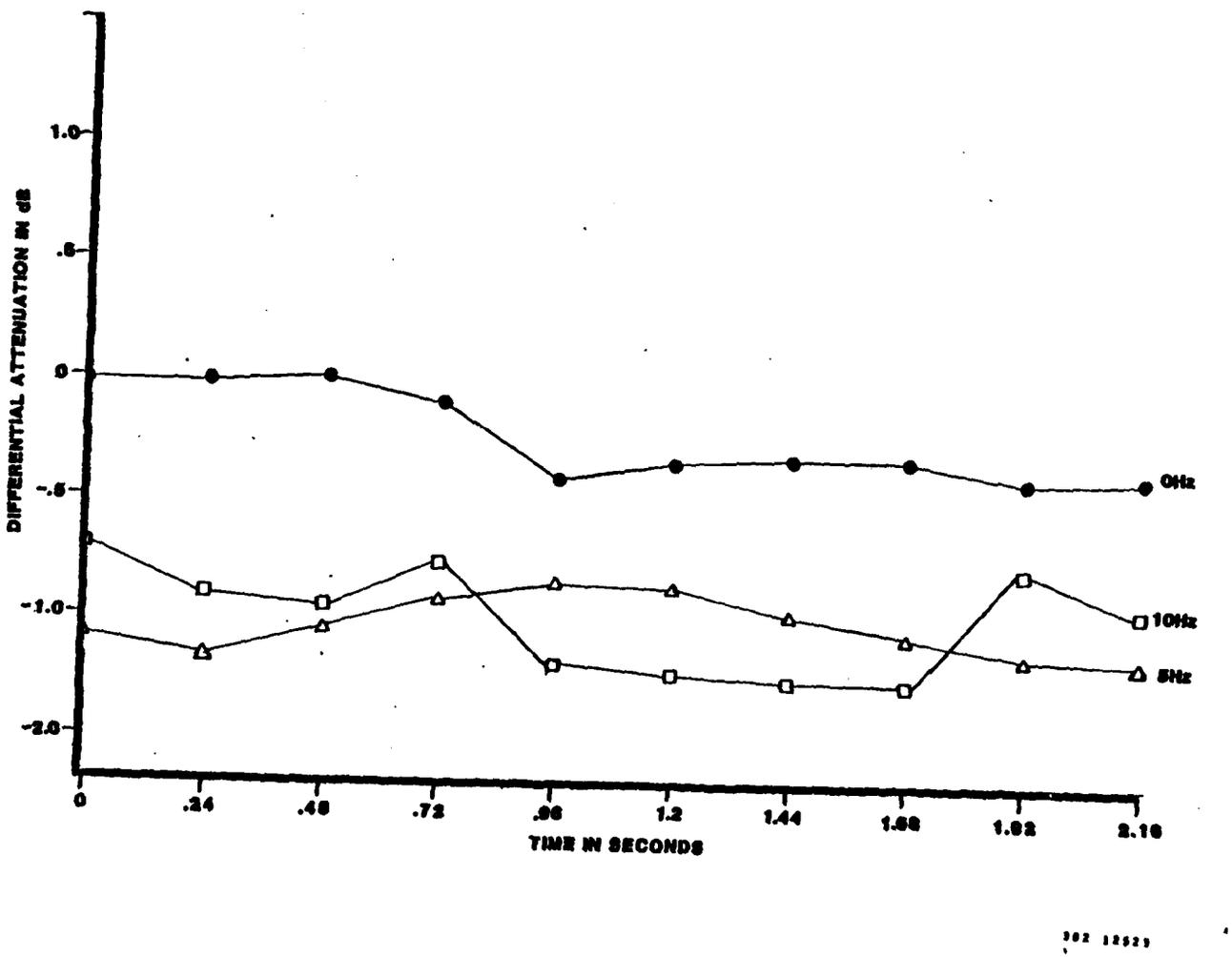

Figure 2.3.2-10. Tension Test EMH-20726c Section 2.

In order to achieve a stable output from the lock-in amplifier, it was necessary to use output filter time constants which attenuated any effects varying at rates in excess of 1 Hz. Therefore, while the strip chart data accurately records the average differential attenuation, it was necessary to devise a different recording system to observe faster time varying effects.

To achieve real time data records, the outputs of the coupler and output detectors were input to a dual channel oscilloscope. The scope traces were then photographed, while the tensile stress was applied to determine the effect on fiber attenuation.

Photographs of the traces for the four fibers tested at 5 Hz and 10 Hz are shown in Figures 2.3.2-11 and 2.3.2-12. The photographs clearly show that the dynamic tensile load had insignificant effects on test fiber transmission.

The photographs also give visual confirmation that the coupler and the output detectors track uniformly. It should be noted that the EMH-20726C coupler exhibits room light effects. This is due to the very low power level coupled from the fiber. The fiber section where the bend was introduced was too weak to

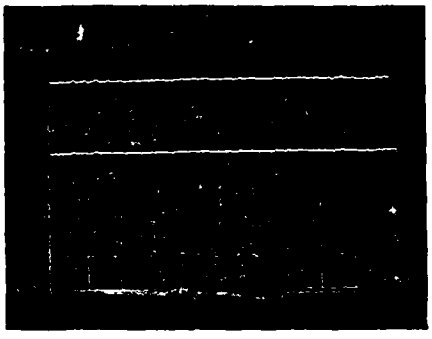

EMT-20721
Horizontal 50 ms/div
Vertical tap voltage, Upper Trace 20 mV/div
Output voltage, Lower Trace 20 mV/div

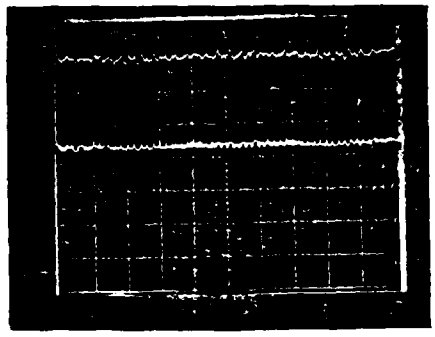

EMT-20793
Horizontal 50 ms/div
Vertical tap voltage, Upper Trace 5 mV/div
Output voltage, Lower Trace 10 mV/div

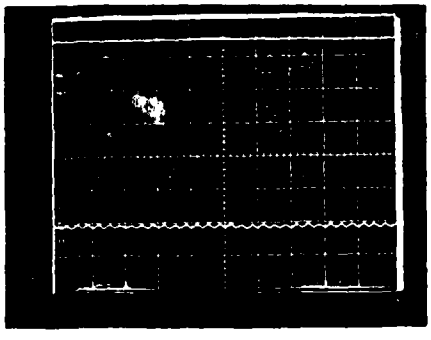

EM-20495
Horizontal 50 ms/div
Vertical tap voltage, Lower Trace 10 mV/div
Output voltage, Upper Trace 50 mV/div

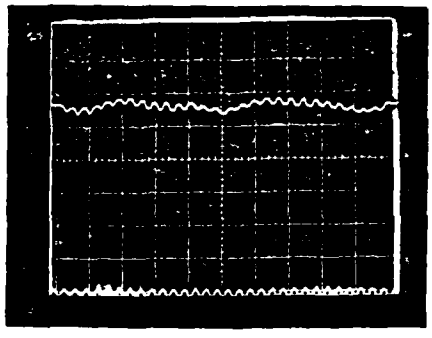

EMH-20726c
Horizontal 50 ms/div
Vertical tap voltage, Lower Trace 5 mV/div
Output voltage, Upper Trace 50 mV/div

Figure 2.3.2-11. Tension Test at 5 Hz.

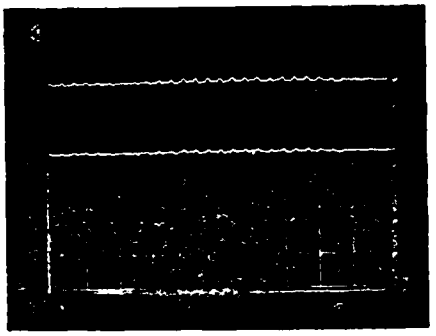

EMT-20721
Horizontal 50 ms/div
Vertical tap voltage, Upper Trace 20 mV/div
Output voltage, Lower Trace 20 mV/div

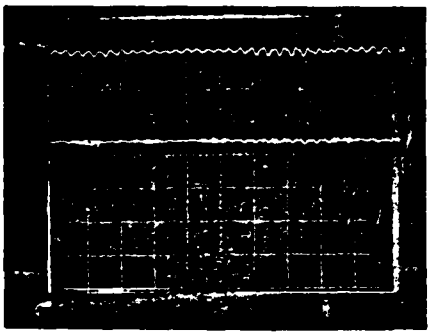

EMT-20793
Horizontal 50 ms/div
Vertical tap voltage, Upper Trace 5 mV/div
Output voltage, Lower Trace 10 mV/div

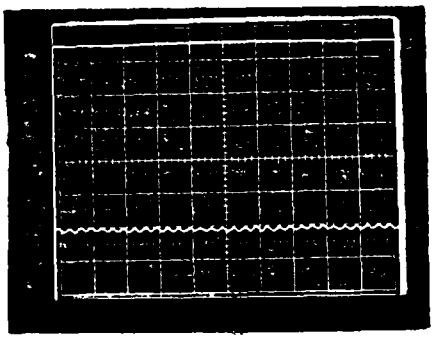

EM-20495
Horizontal 50 ms/div
Vertical tap voltage, Lower Trace 10 mV/div
Output voltage, Upper Trace 50 mV/div

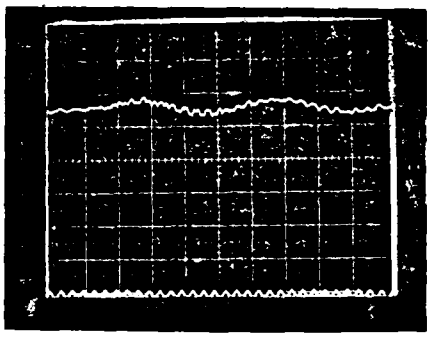

EMH-20726c
Horizontal 50 ms/div
Vertical tap voltage, Lower Trace 5 mV/div
Output voltage, Upper Trace 50 mV/div

Figure 2.3.2-12. Tension Test at 10 Hz.

support the small bend required to couple higher power fractions from a high NA fiber.

2.3.3 Dynamic Twist Test

The equipment of Figure 2.3.3-1 was used to simulate the effects of a dynamic twist stress on a deployed single mode fiber. The apparatus is attached to the sliding carriage of Figure 2.3.2-1. The use of the sliding carriage as a common drive mechanism eliminates significant assembly and disassembly time between tests.

The test fiber is routed through the pin vise and secured. The fiber is also secured in the buffered jaws of a vise at a distance of 19 cm (7.5 in) from the pin vise.

The ±2.5 cm (±1.0 in) linear translation of the rack produces a ±90° twist in the 19 cm section.

As in the dynamic tension test, two groups of tests were conducted at translation frequencies of 0, 5, and 10 Hz.

The first test monitored the average differential attenuation with the equipment of Figure 2.3.2-2. The data obtained is shown in Figures 2.3.3-2 through 2.3.3-9. The data shows very small deviations in fiber attenuation during the test for

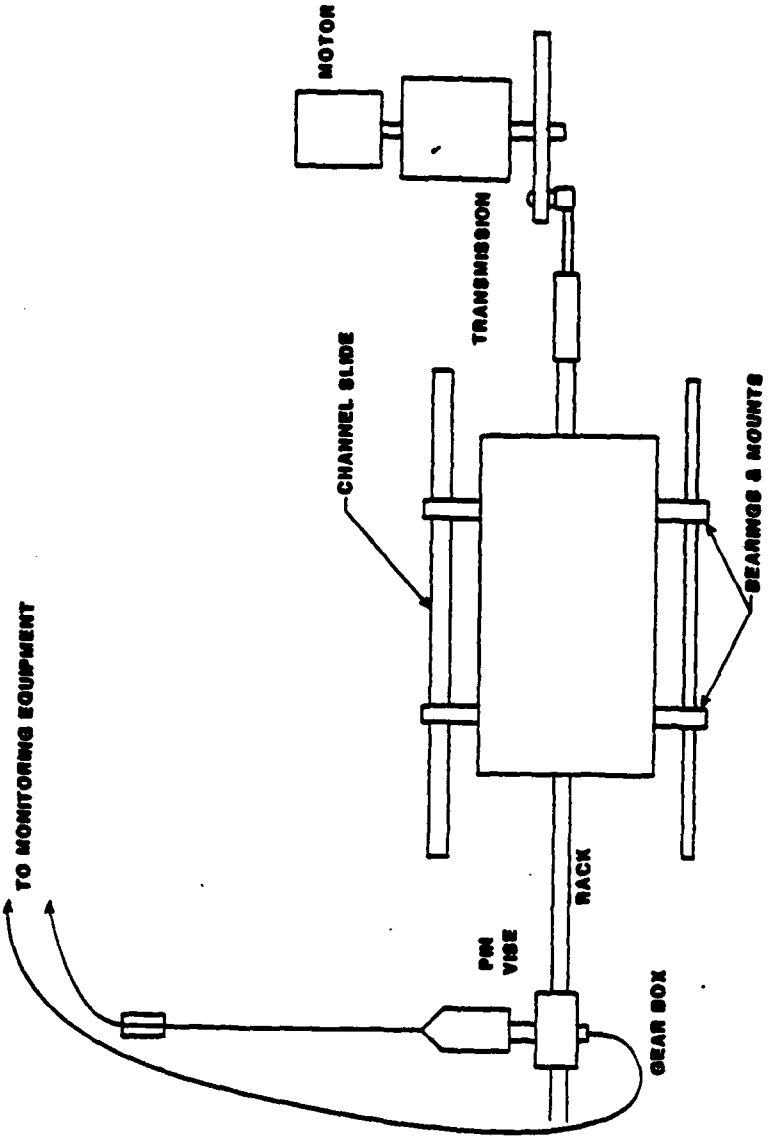

Figure 2.3.3-1. Dynamic Twist Test Apparatus.

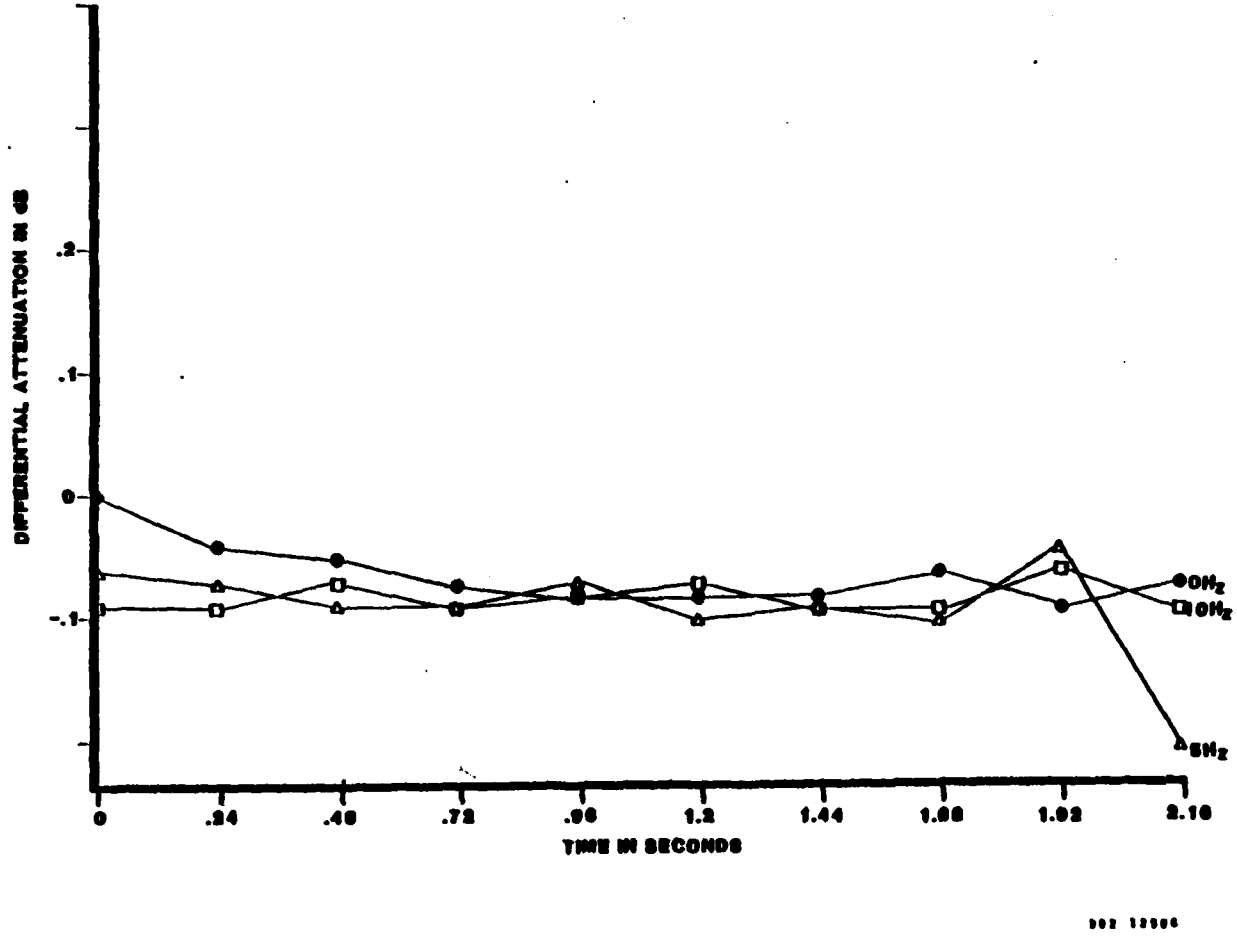

Figure 2.3.3-2. Twist Test EMT-20721 Section 1.

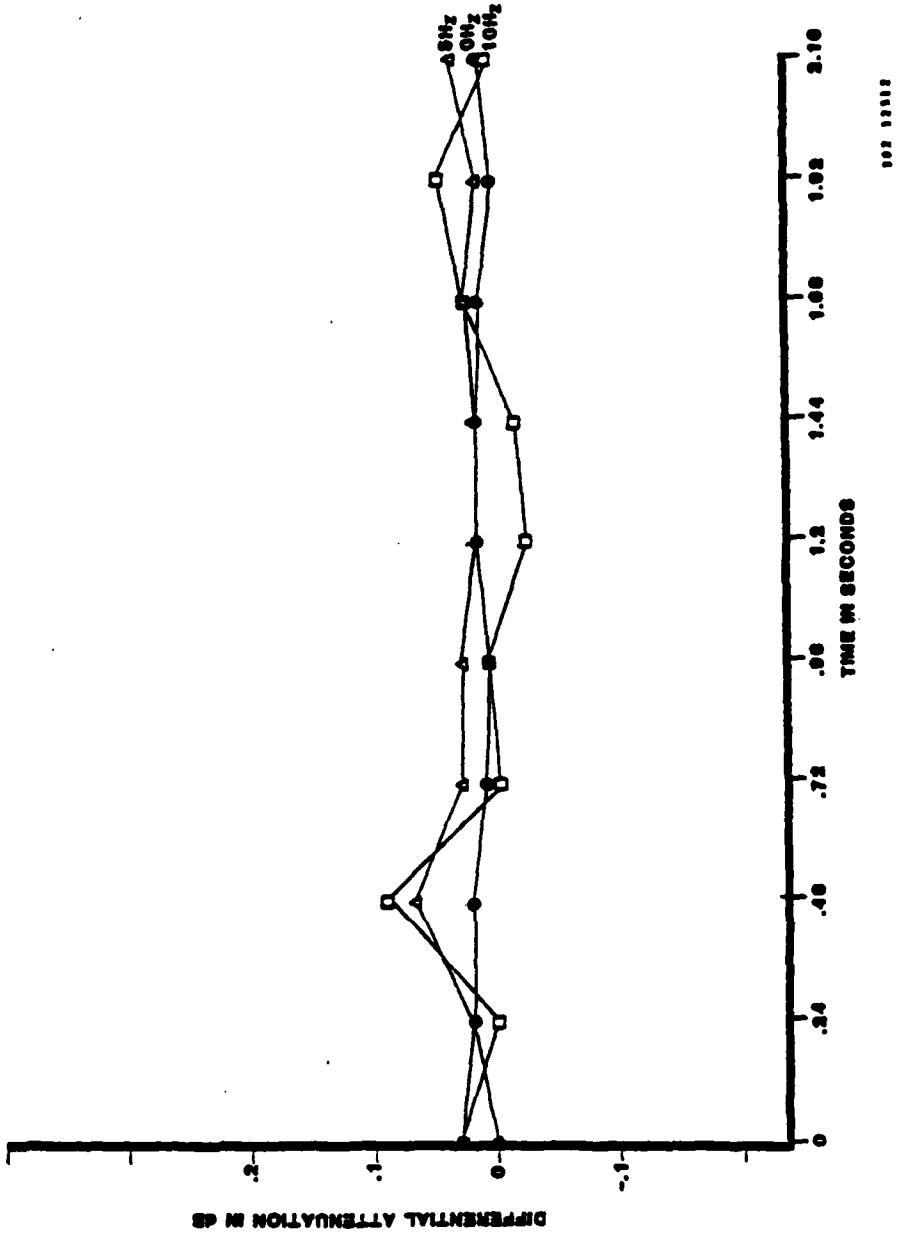

Figure 2.3.3-3. Twist Test EMT-20721 Section 2.

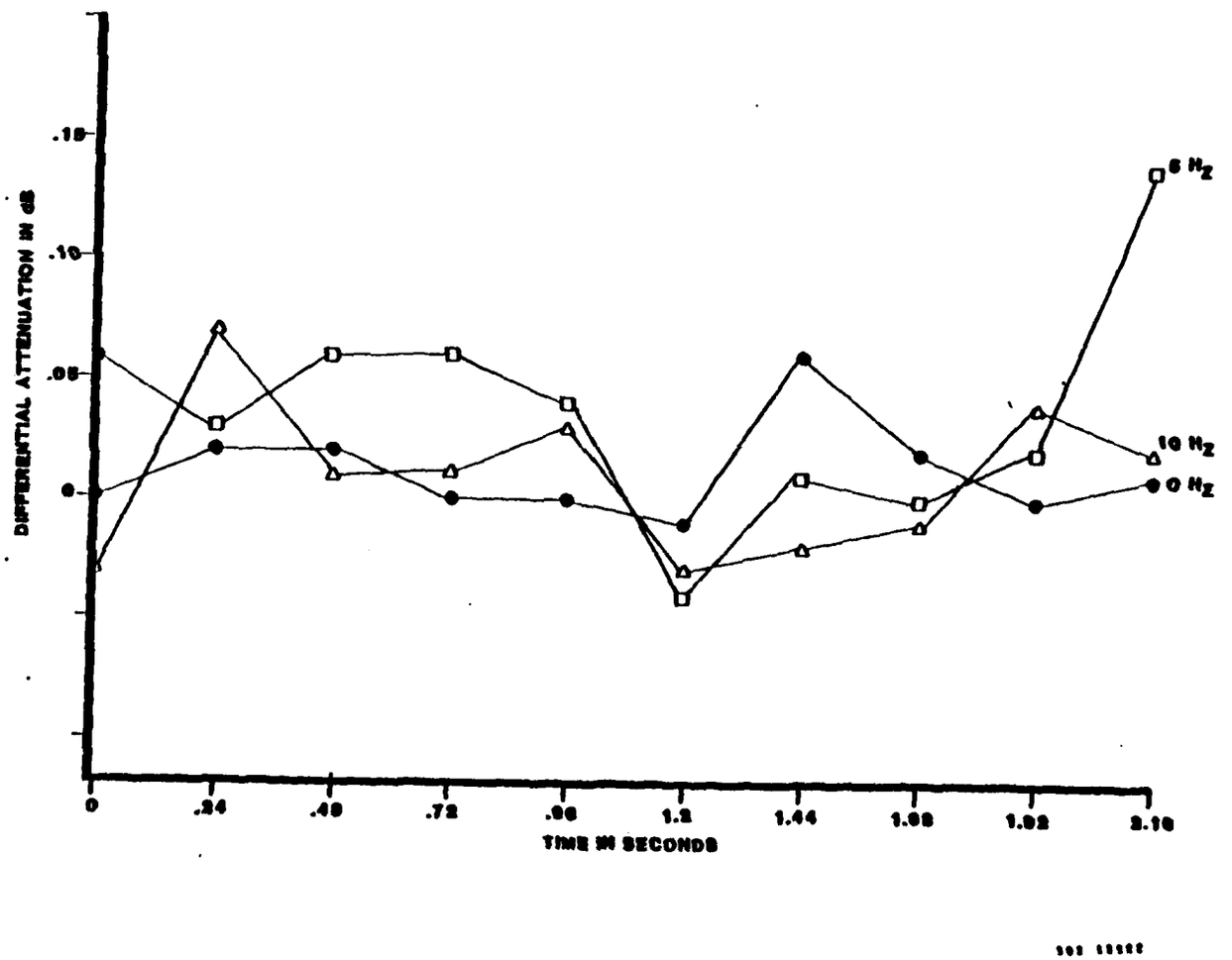

Figure 2.3.3-4. Twist Test EMT-20793 Section 1.

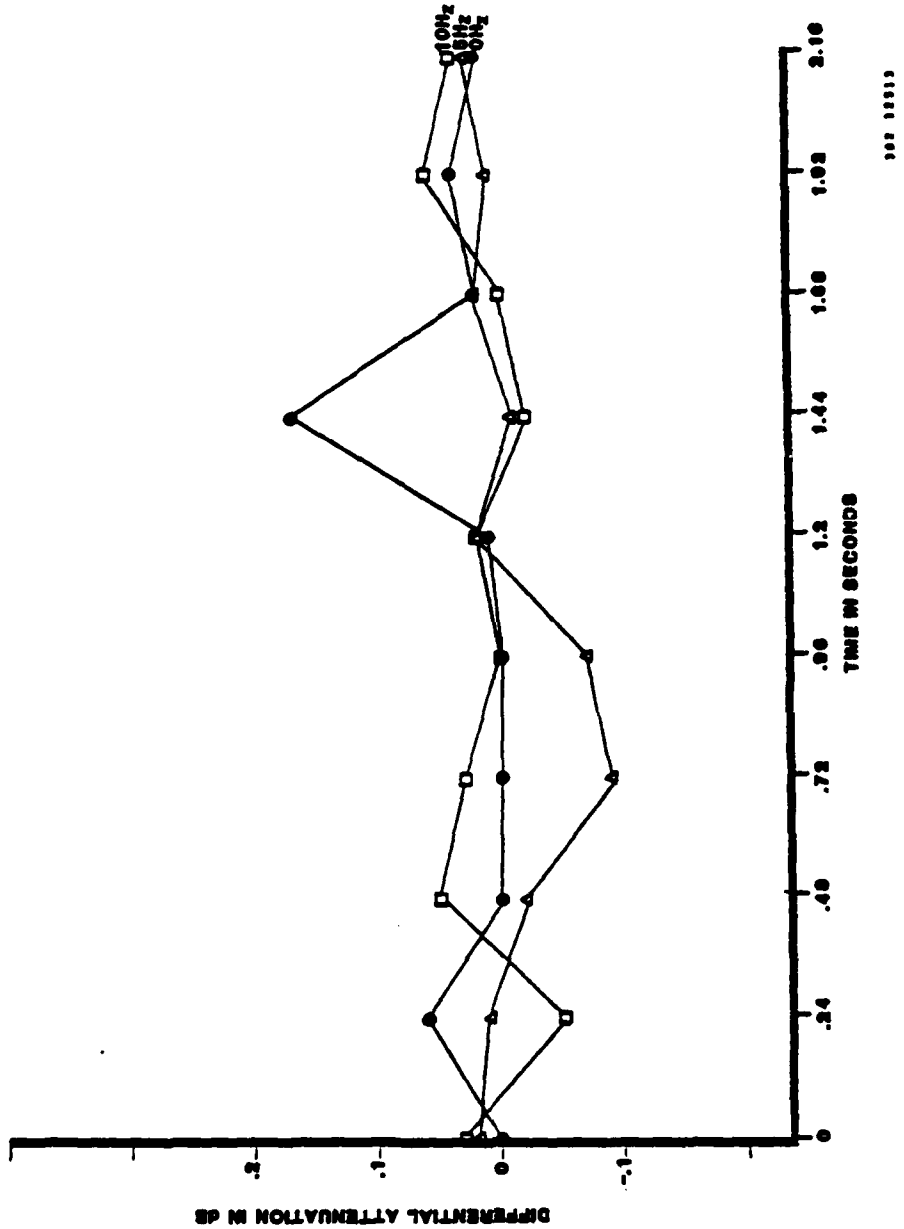

Figure 2.3.3-5. Twist Test EMT-20793 Section 2.

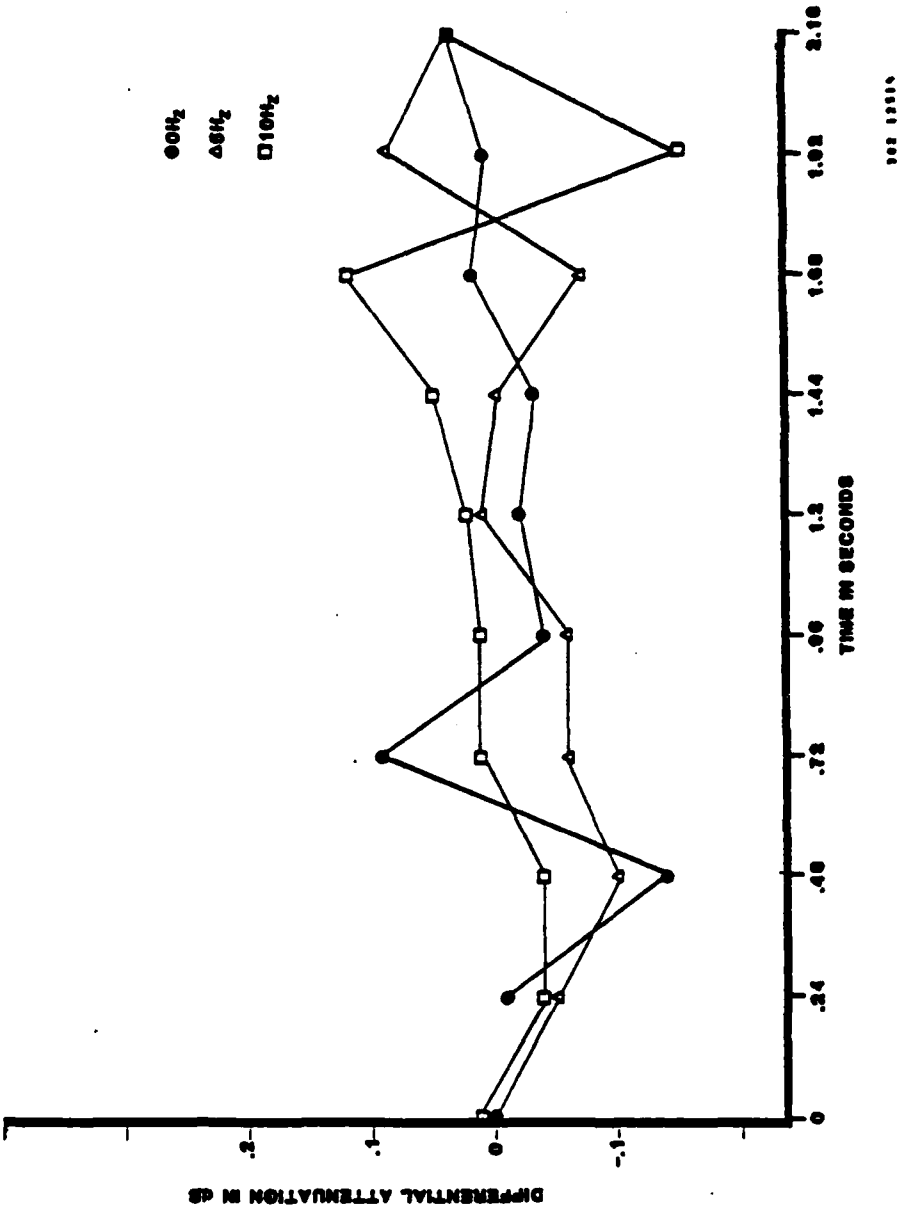

Figure 2.3.3-6. Twist Test EM-20495 Section 1.

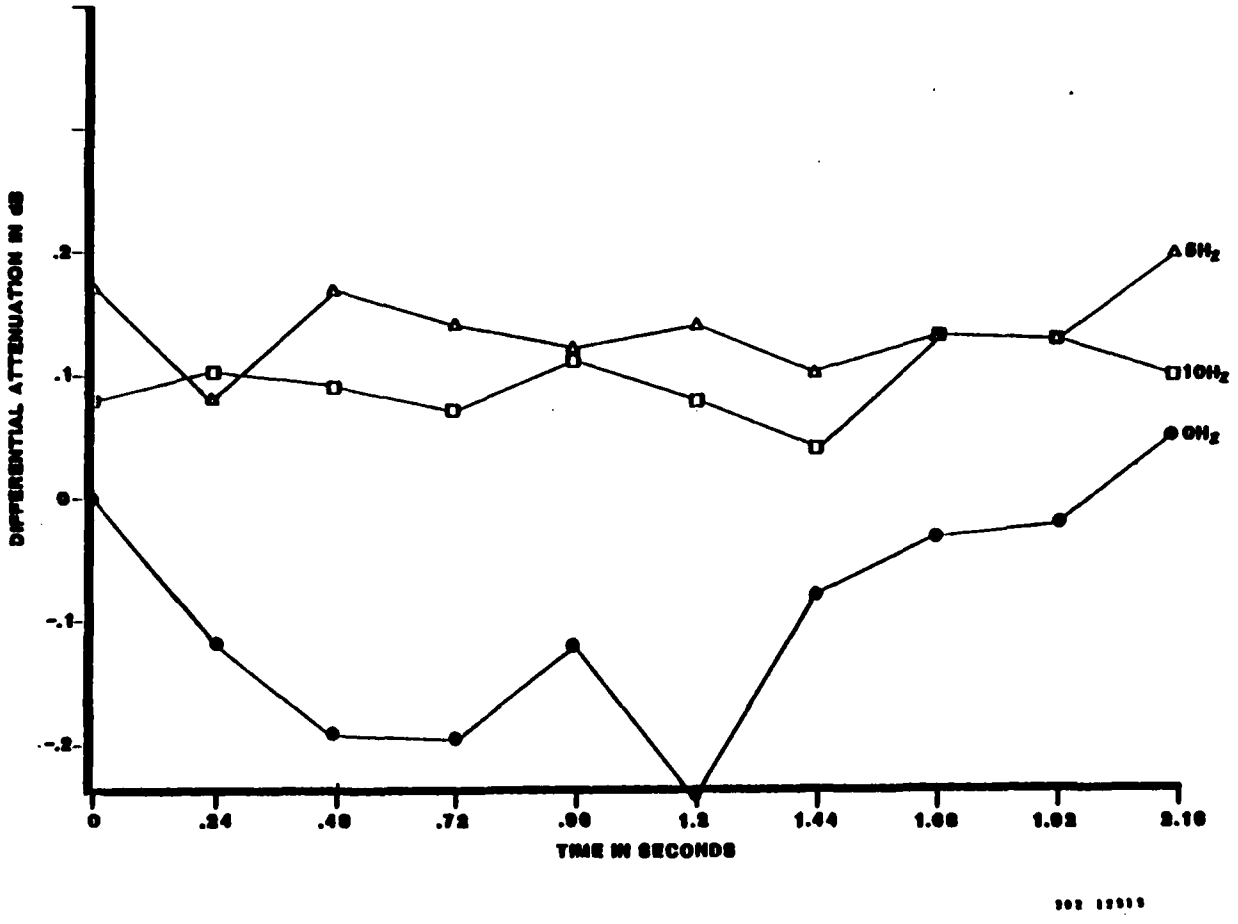

Figure 2.3.3-7. Twist Test EM-20495 Section 2.

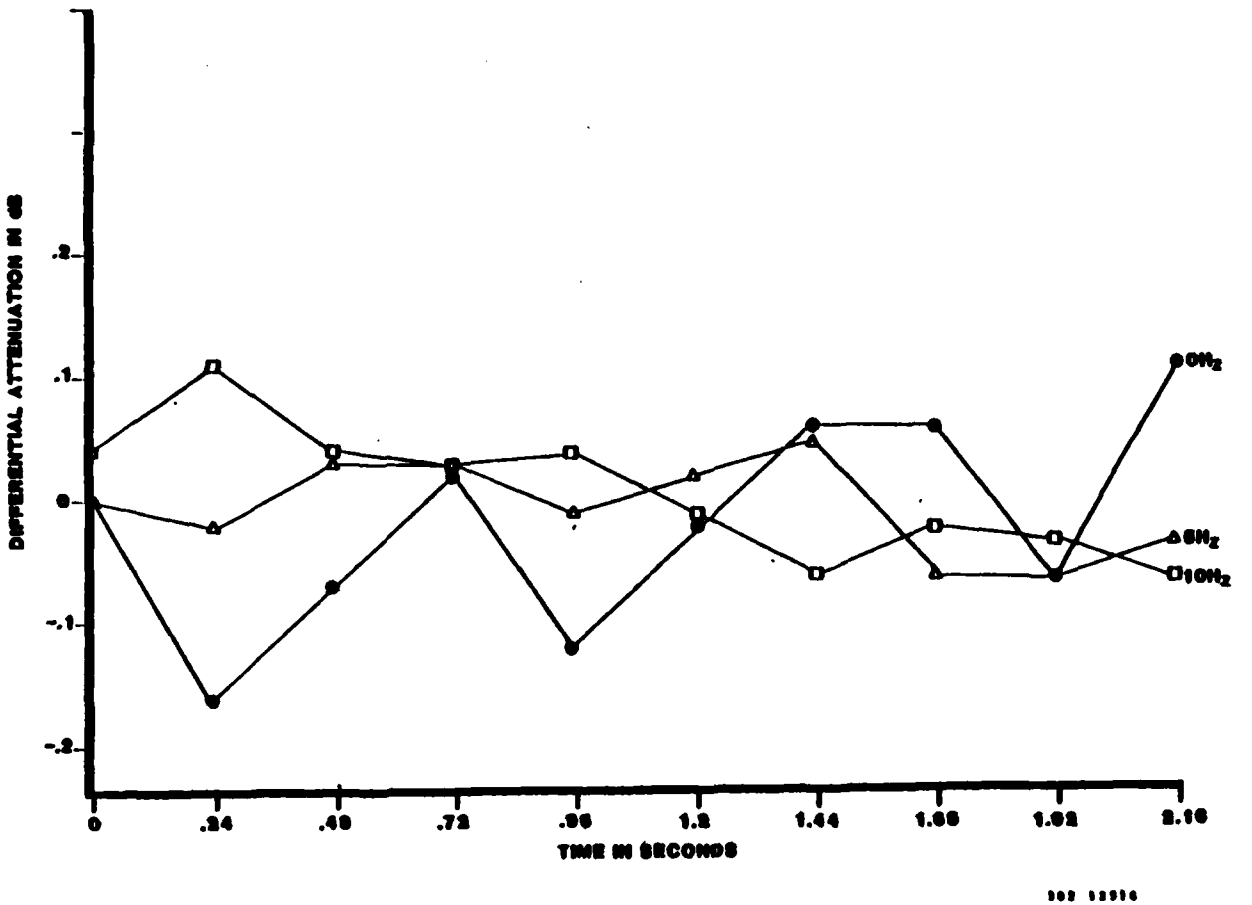

Figure 2.3.3-8. Twist Test EMH-20726c Section 1.

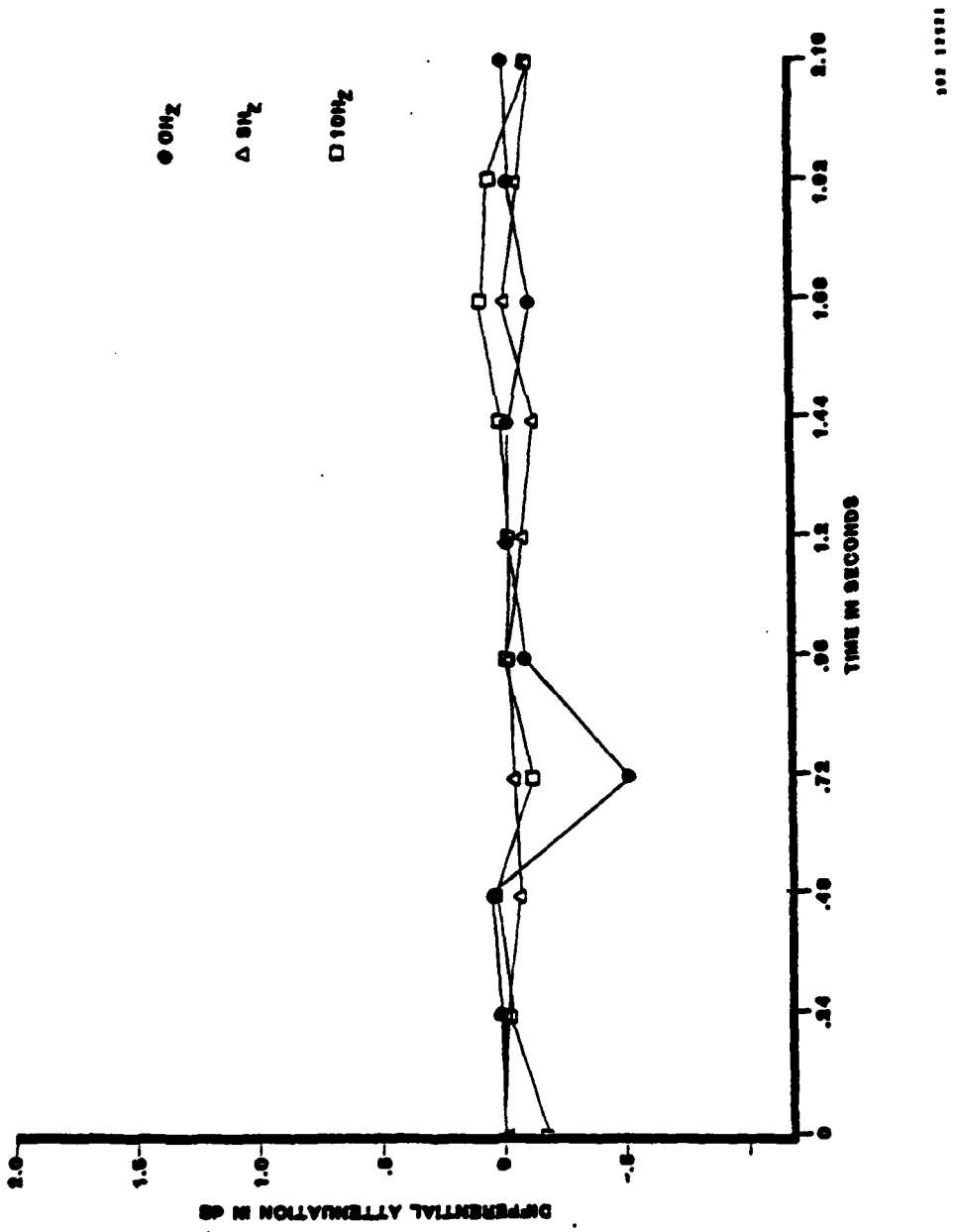

Figure 2.3.3-9. Twist Test EMH-20726c Section 2.

all fiber types.

To verify that no variations in the output were masked by the low bandwidth of the lock-in amplifier, the tests were repeated using oscilloscope photographs to record the waveforms. The photos obtained, shown in Figures 2.3.3-10 and 2.3.3-11, indicate no higher frequency effects.

2.3.4 Dynamic Bend Tests

The equipment of Figure 2.3.4-1 was used to apply dynamic bend stress to test fibers. The apparatus is driven by the sliding carriage assembly of Figure 2.3.2-1.

Based on results obtained in static bending tests of single mode fibers, dynamic bend effects were expected to be sensitive to mandrel diameters. Therefore, mandrel diameters of 1.27 cm (0.5 in) and 0.64 cm (0.25 in) were used. Differential attenuation was monitored while the frequency of the $\pm 90^{o}$ bend motion was varied between 0, 5, and 10 Hz.

The data from the first set of tests, where the average differential attenuation was recorded, are shown in Figures 2.3.4-2 through 2.3.4-9. As in static tests reported elsewhere, the bending induced loss increased with decreasing mandrel diameter and decreasing fiber NA.

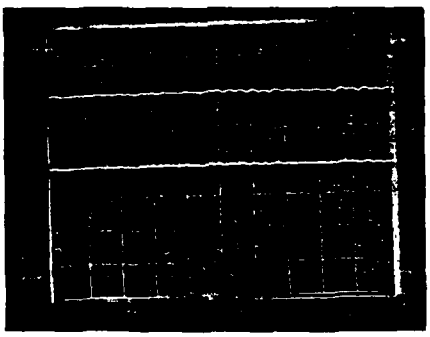

EMT-20721
Horizontal 50 ms/div
Vertical tap voltage, Upper Trace 20 mV/div
Output voltage, Lower Trace 20 mV/div

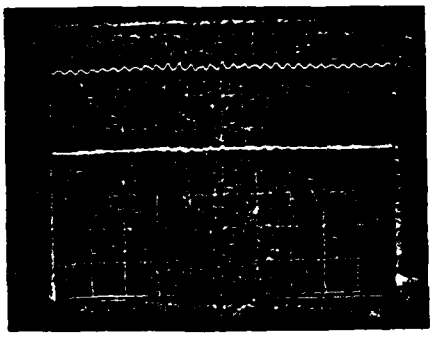

EMT-20793
Horizontal 50 ms/div
Vertical tap voltage, Upper Trace 5 mV/div
Output voltage, Lower Trace 10 mV/div

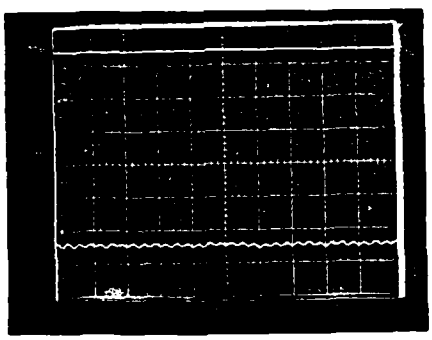

EM-20495
Horizontal 50 ms/div
Vertical tap voltage, Lower Trace 10 mV/div
Output voltage, Upper Trace 50 mV/div

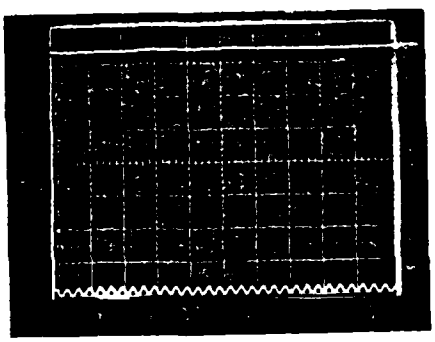

EMH-20726c
Horizontal 50 ms/div
Vertical tap voltage, Lower Trace 5 mV/div
Output voltage, Upper Trace 50 mV/div

Figure 2.3.3-10. Twist Test at 5 Hz.

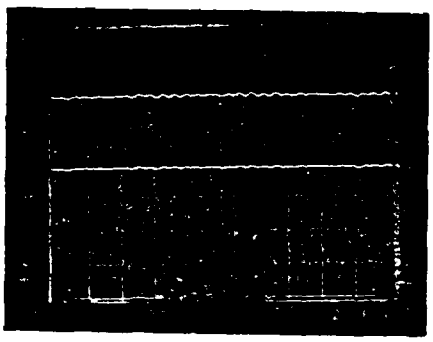

EMT-20721
Horizontal 50 ms/div
Vertical tap voltage, Upper Trace 20 mV/div
Output voltage, Lower Trace 20 mV/div

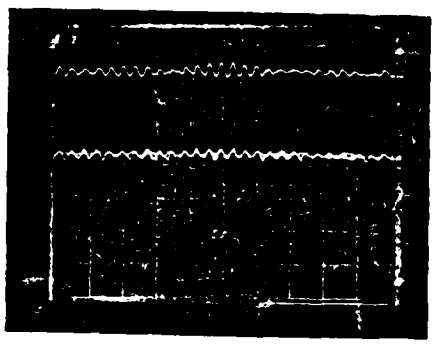

EMT-20793
Horizontal 50 ms/div
Vertical tap voltage, Upper Trace 5 mV/div
Output voltage, Lower Trace 10 mV/div

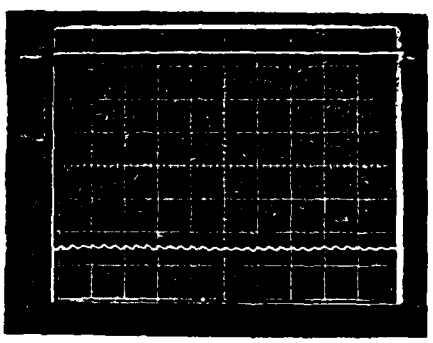

EM-20495
Horizontal 50 ms/div
Vertical tap voltage, Lower Trace 10 mV/div
Output voltage, Upper Trace 50 mV/div

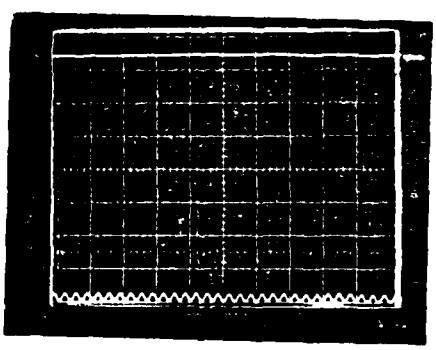

EMH-20726c
Horizontal 50 ms/div
Vertical tap voltage, Lower Trace 5 mV/div
Output voltage, Upper Trace 50 mV/div

Figure 2.3.3-11. Twist Test at 10 Hz.

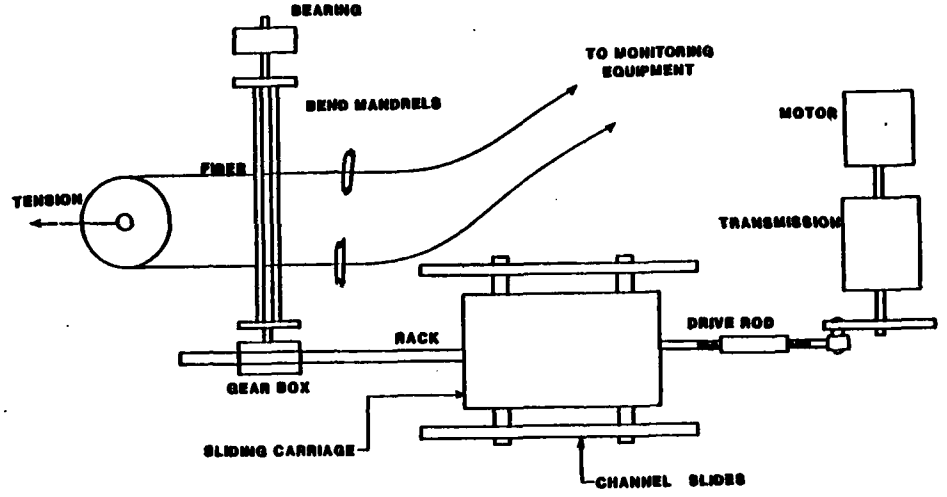

Figure 2.3.4-1. Dynamic Bend Test Apparatus.

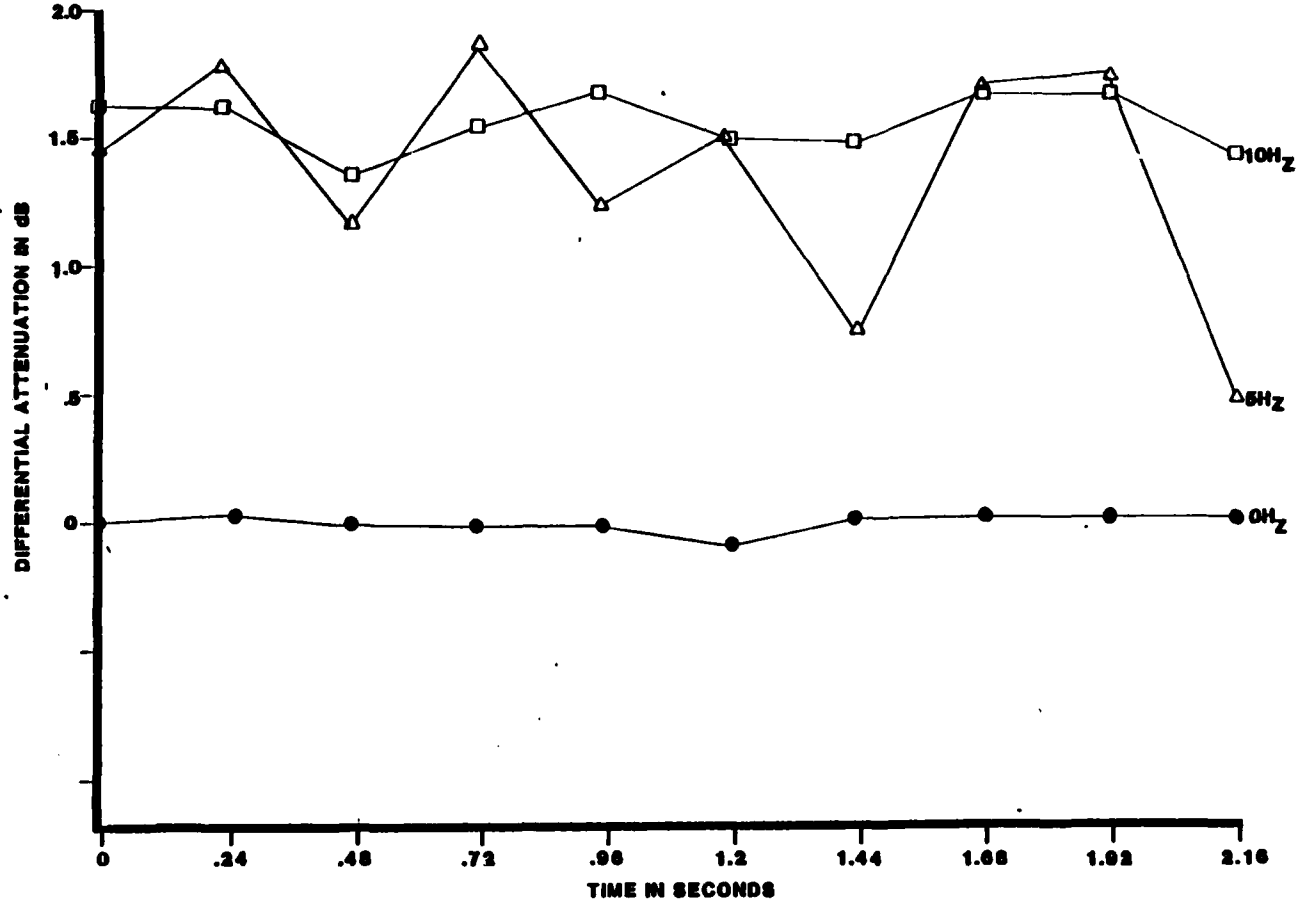

Figure 2.3.4-2.1. Bend Test 6.4 mm Mandrel EMT-20721 Section 1.

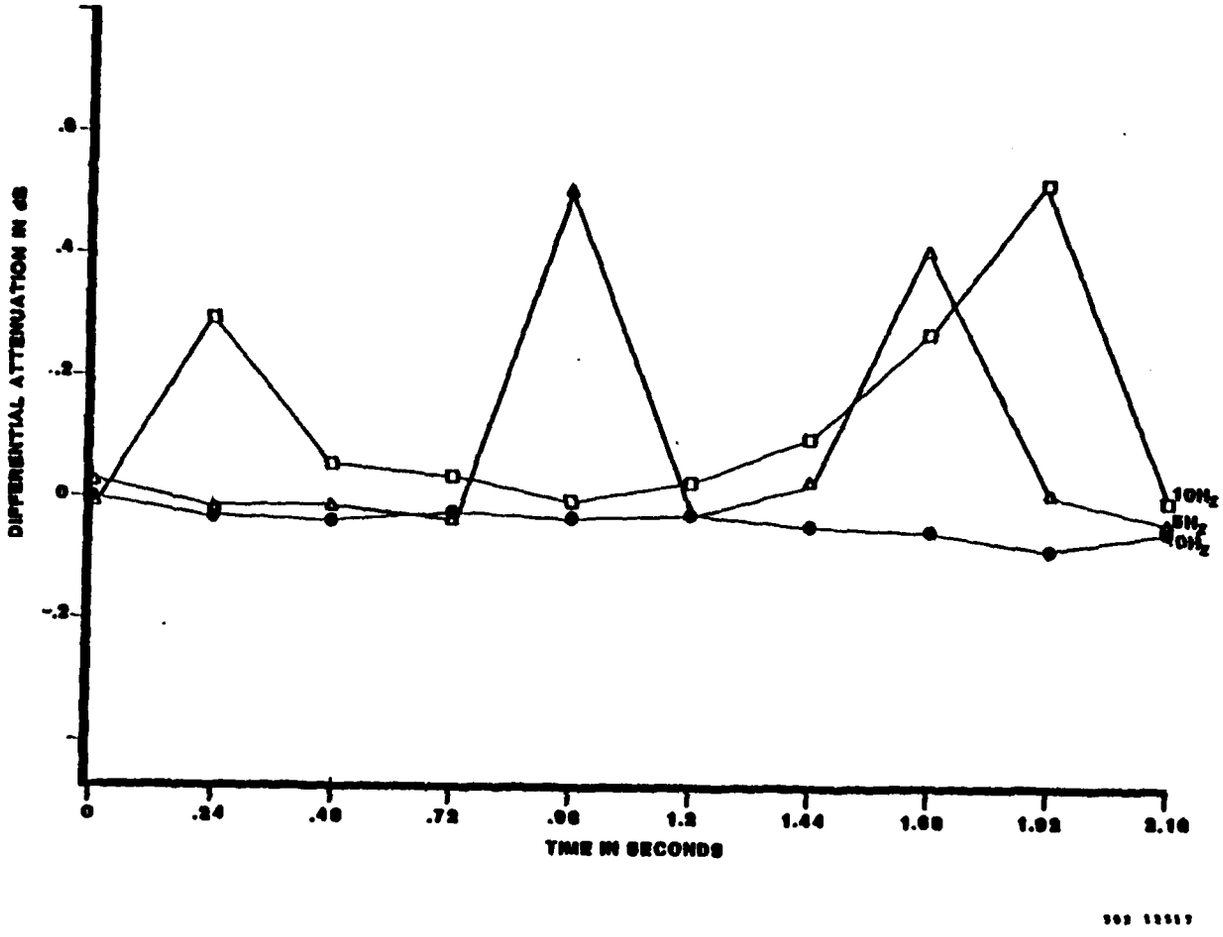

Figure 2.3.4-2.2. Bend Test 12.7 mm Mandrel EMT-20721 Section 1.

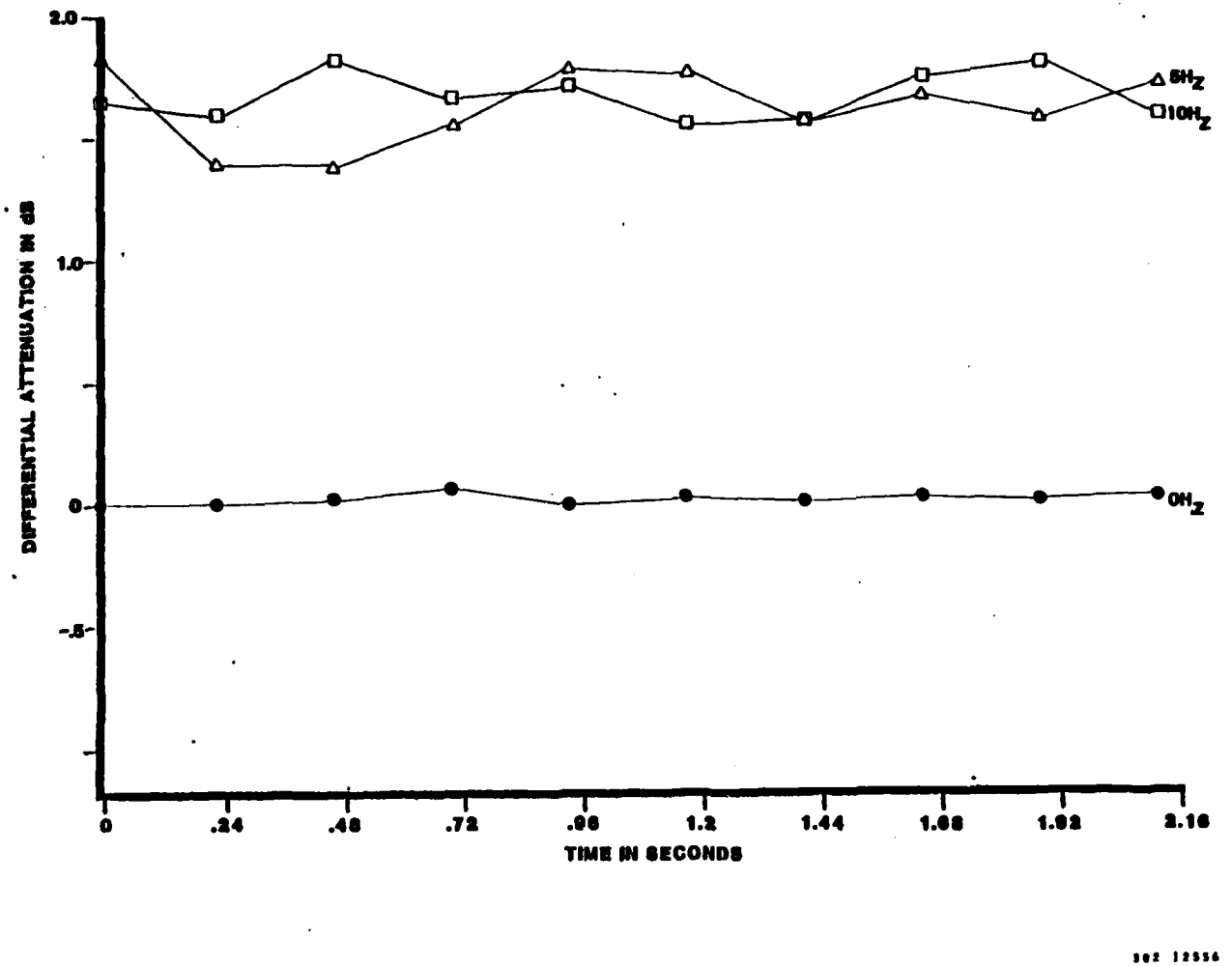

Figure 2.3.4-3.1. Bend Test 6.4 mm Mandrel EMT-20721 Section 2.

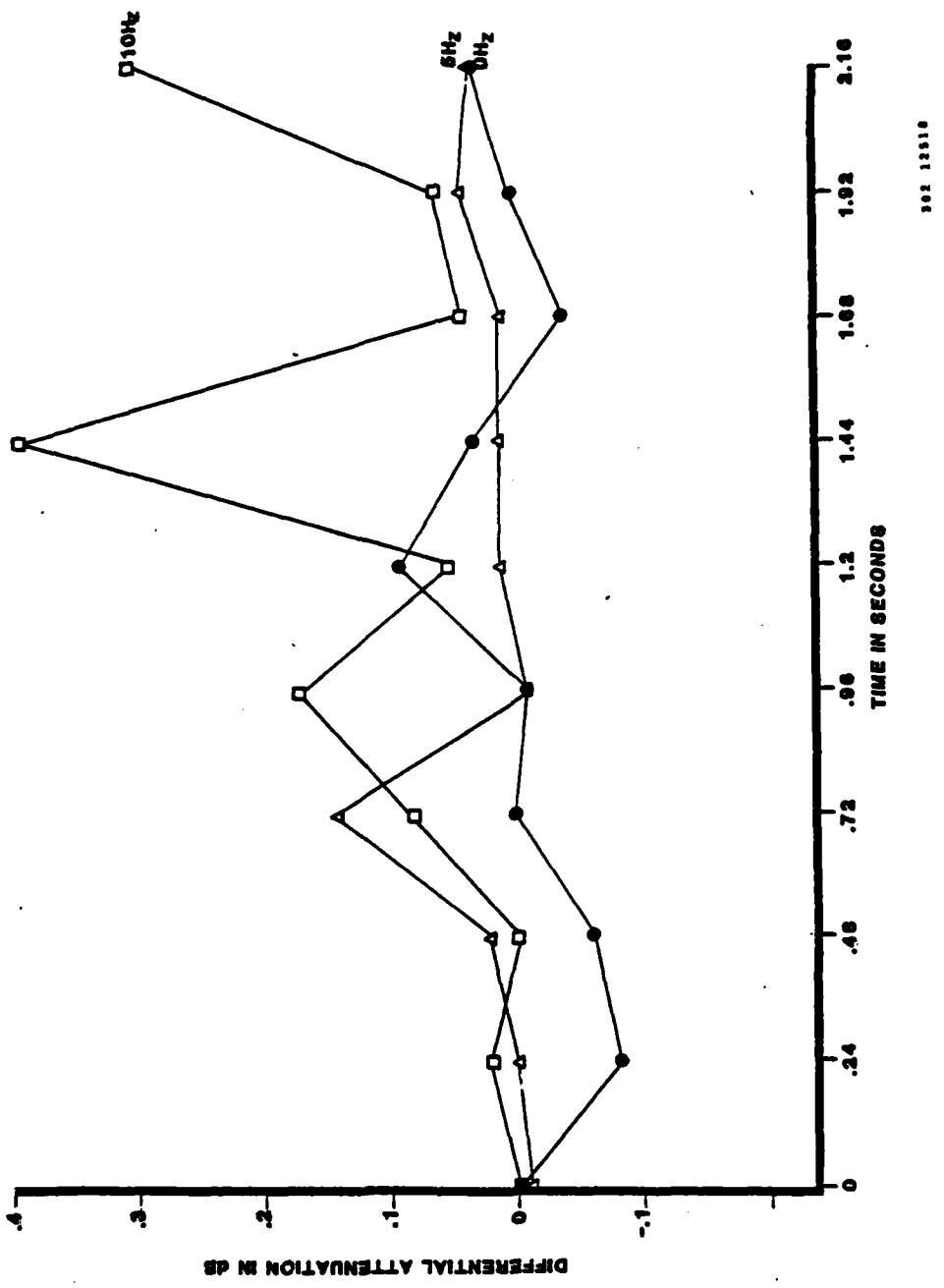

Figure 2.3.4-3.2. Bend Test 12.7 mm Mandrel EMT-20721 Section 2.

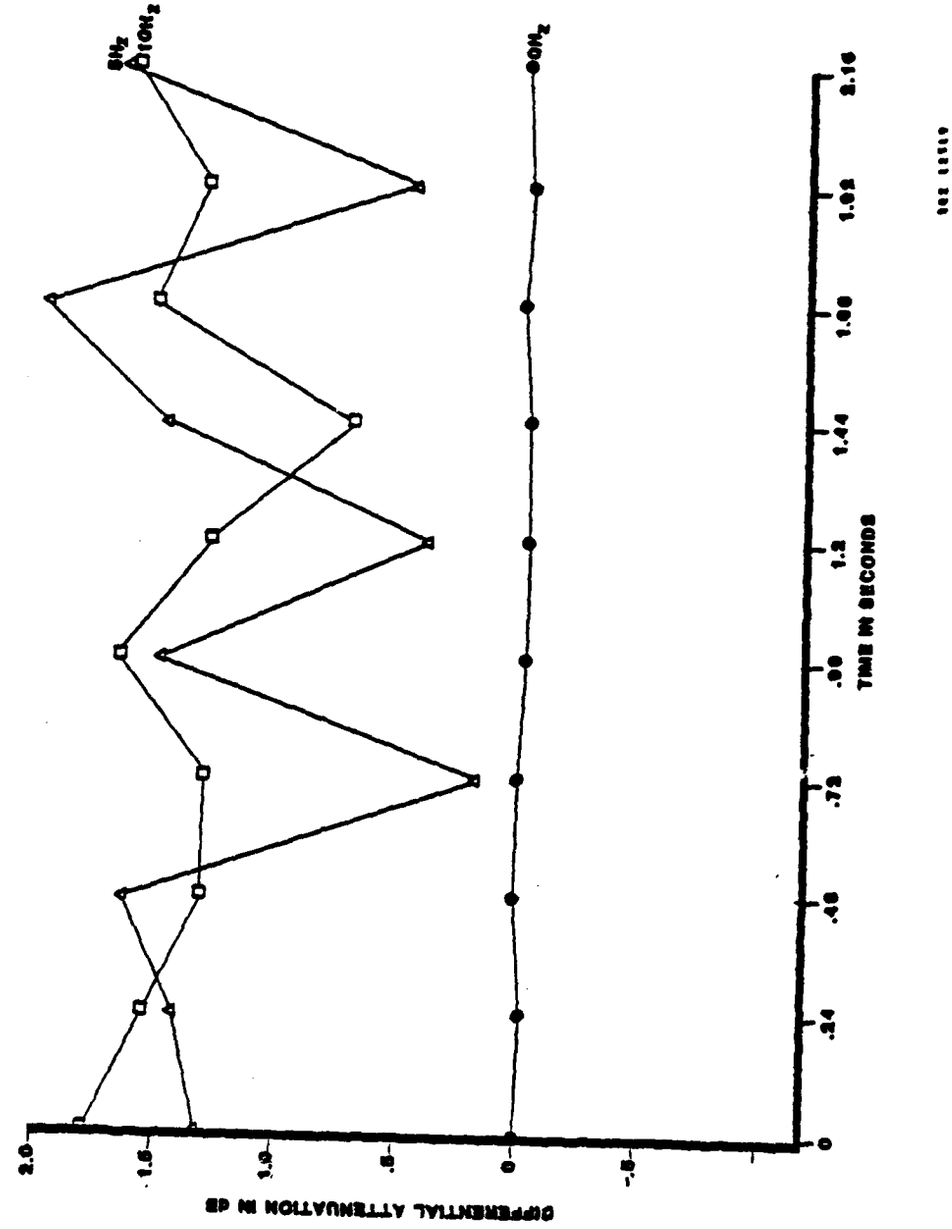

Figure 2.3.4-4.1. Bend Test 6.4 mm Mandrel EMT-20793 Section 1.

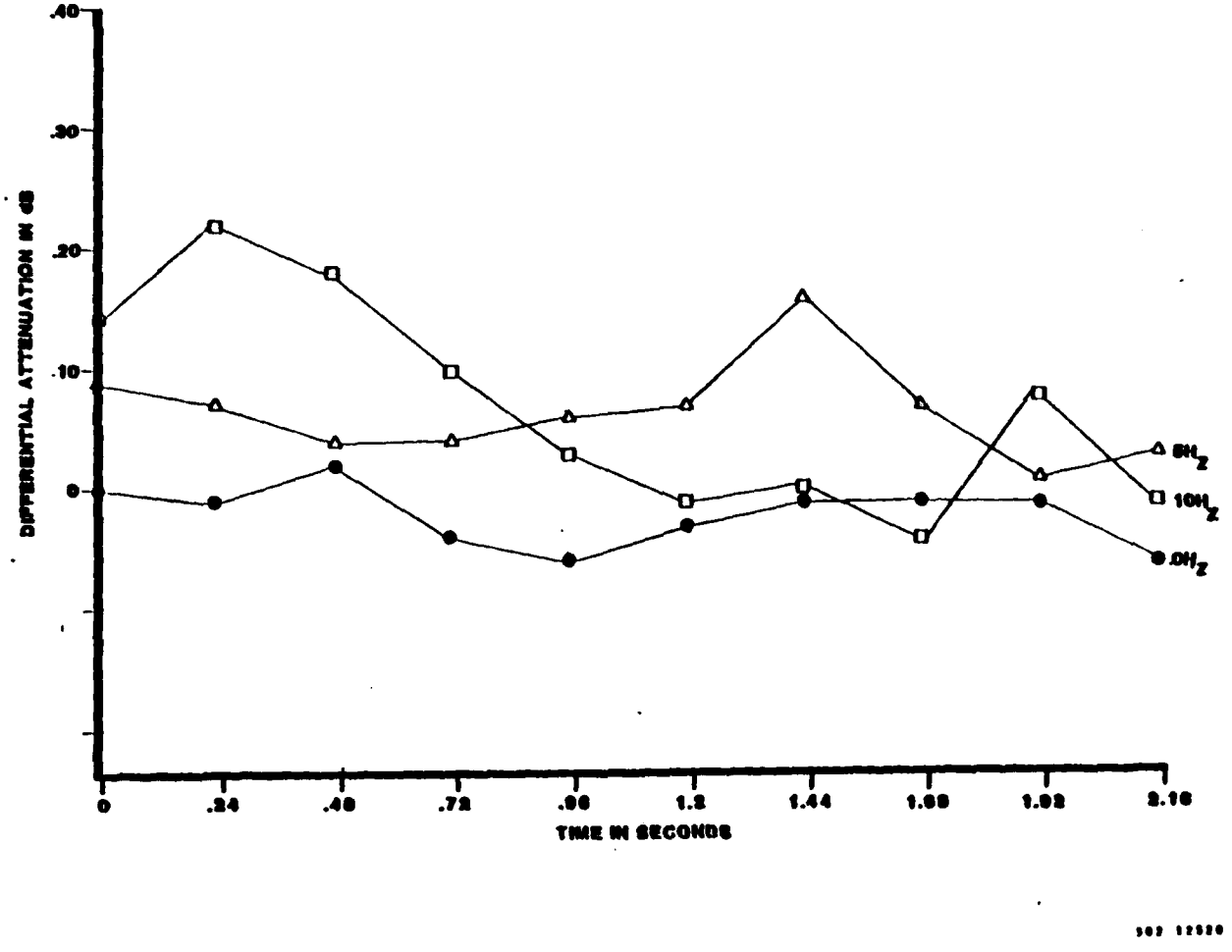

Figure 2.3.4-4.2. Bend Test 12.7 mm Mandrel EMT-20793 Section 1.

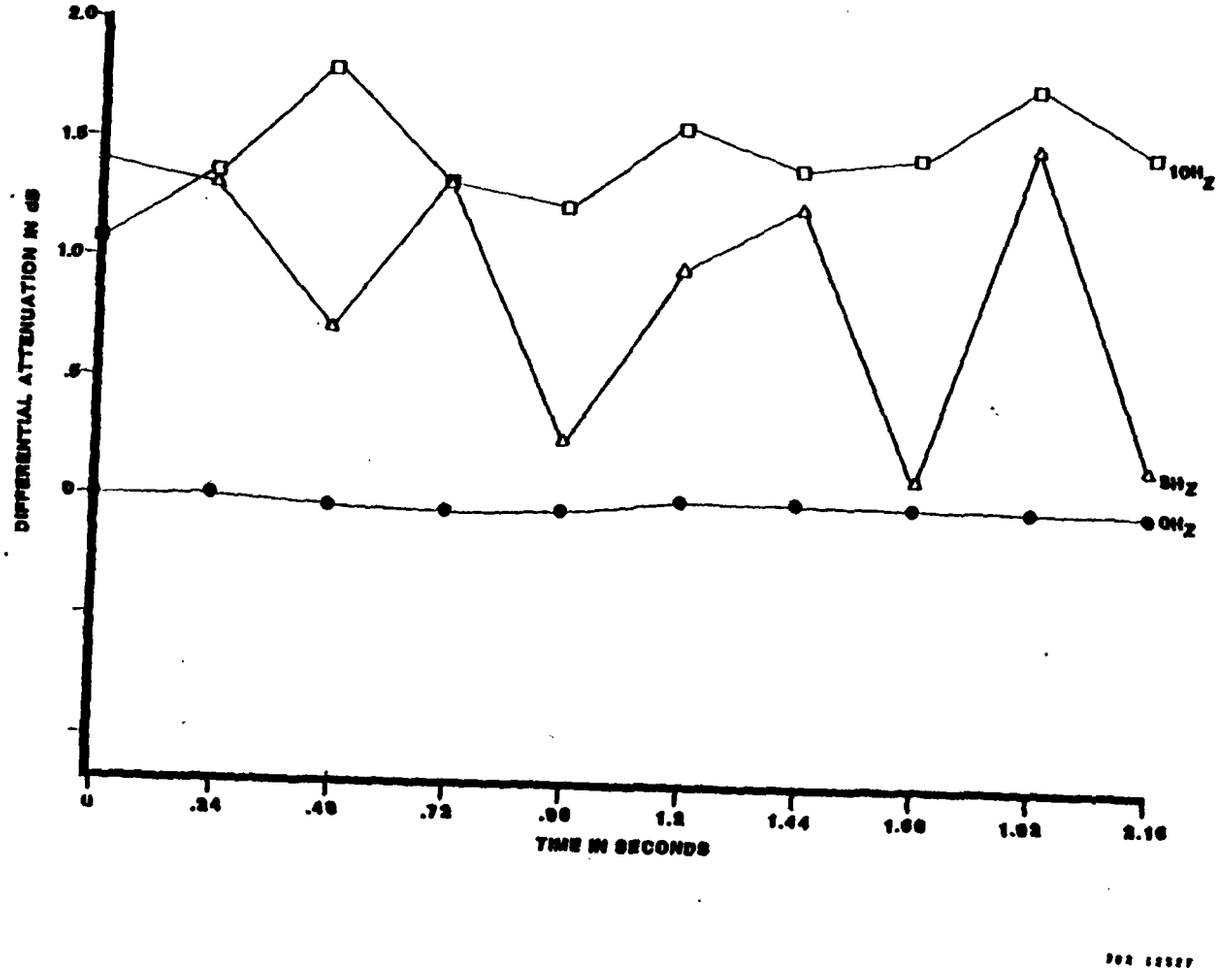

Figure 2.3.4-5.1. Bend Test 6.4 mm Mandrel EMT-20793 Section 2.

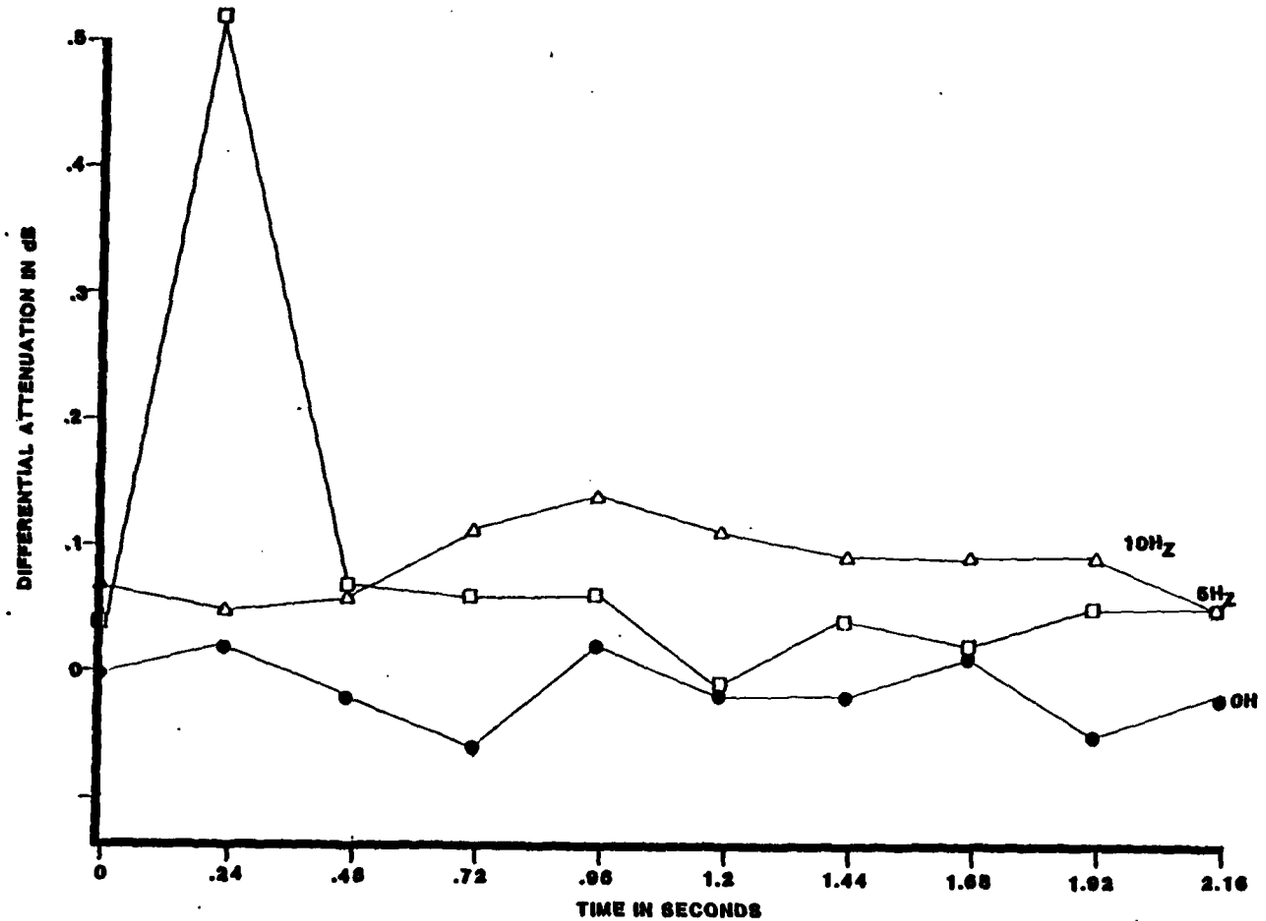

Figure 2.3.4-5.2. Bend Test 12.7 mm Mandrel EMT-20793 Section 2.

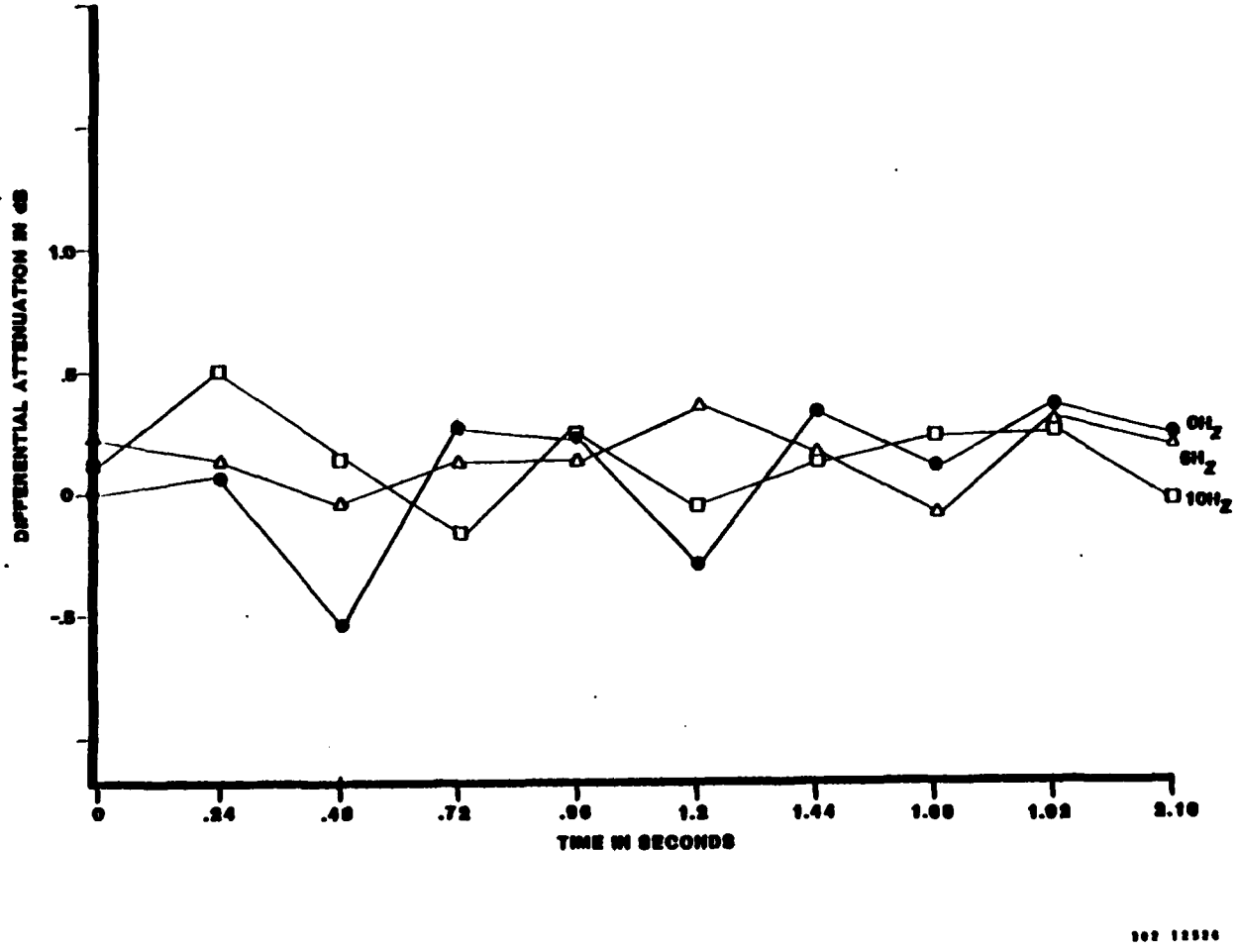

Figure 2.3.4-6.1. Bend Test 6.4 mm Mandrel EM-20495 Section 1.

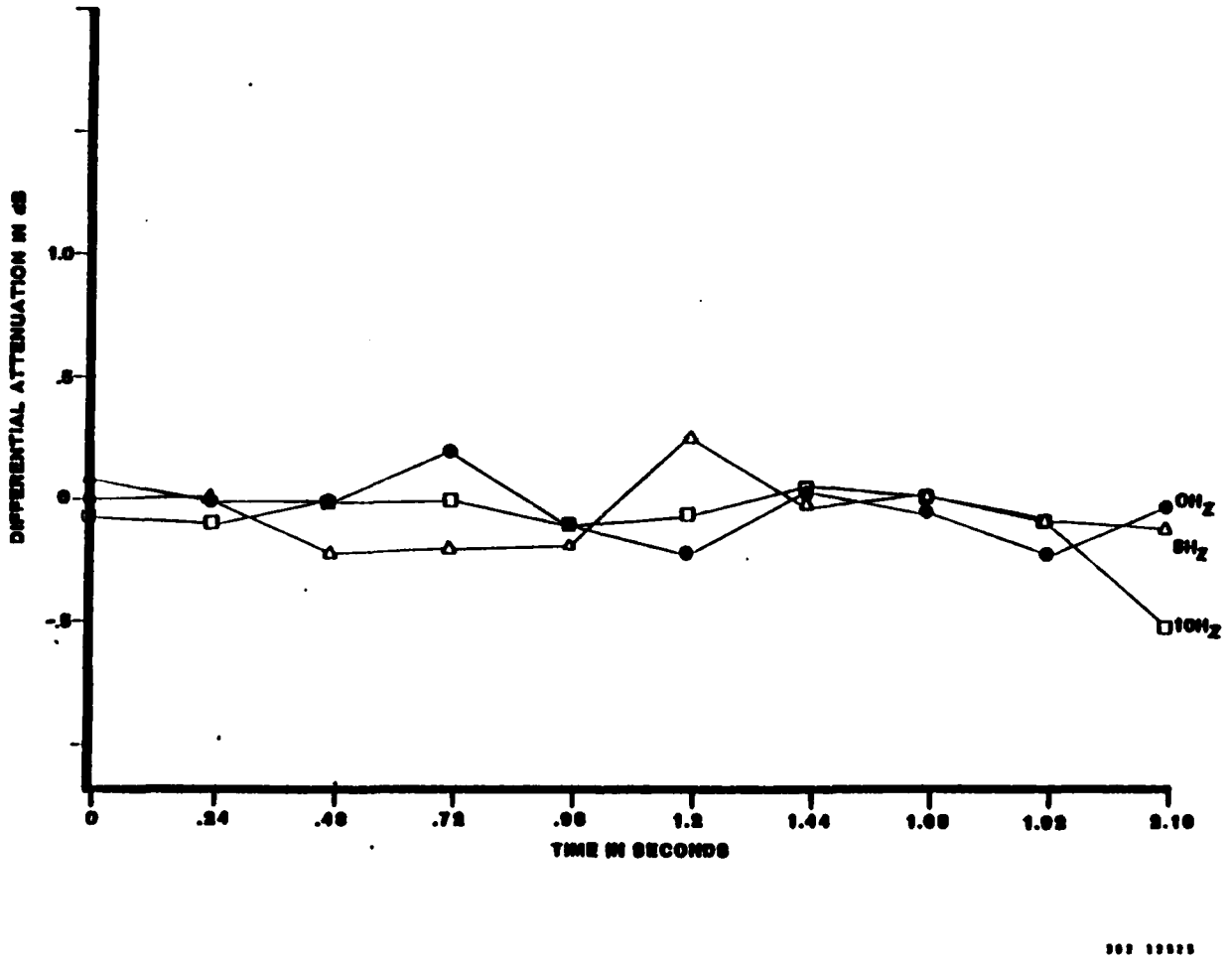

Figure 2.3.4-6.2. Bend Test 12.7 mm Mandrel EM-20495 Section 1.

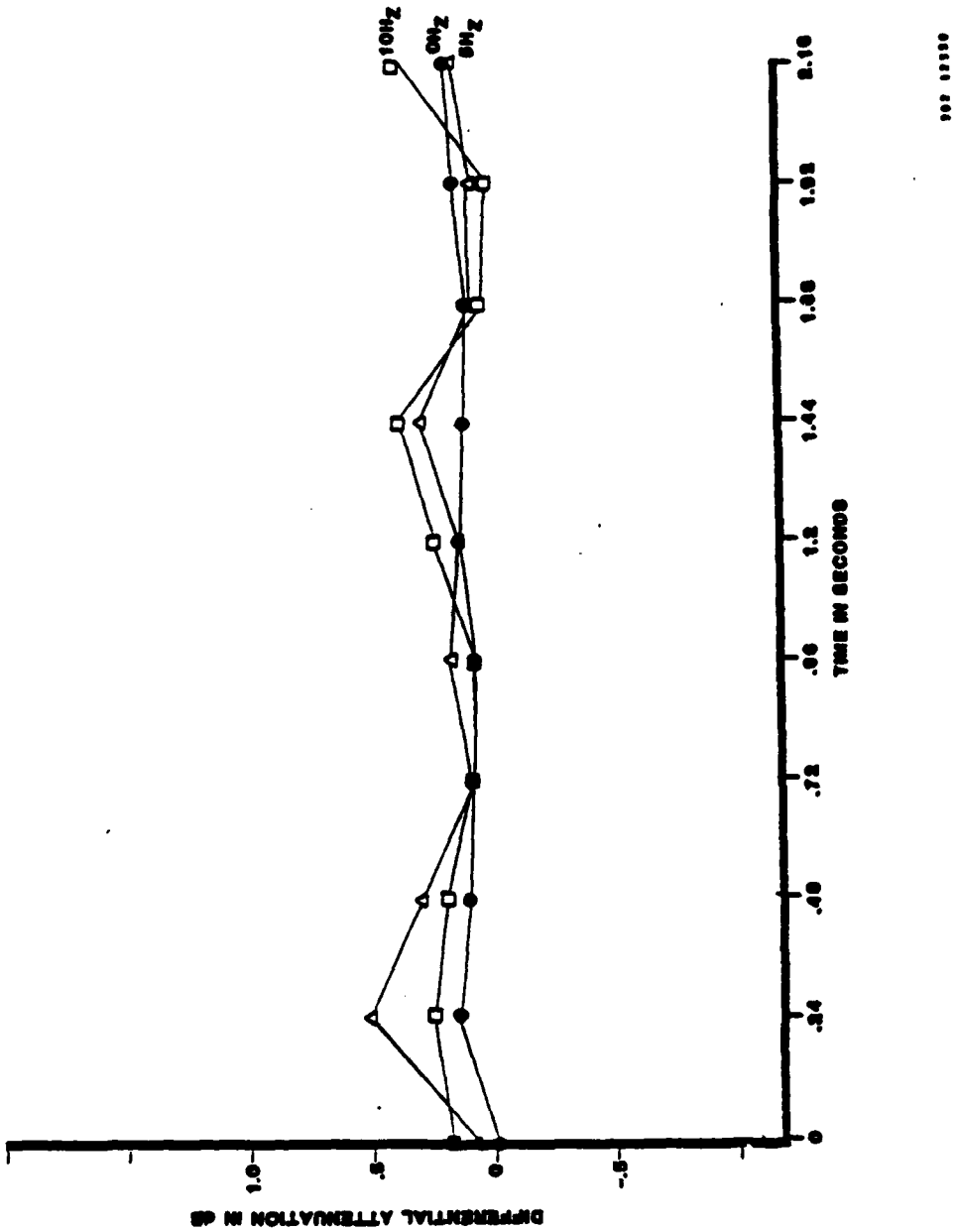

Figure 2.3.4-7.2. Bend Test 12.7 mm Mandrel EM-20495 Section 2.

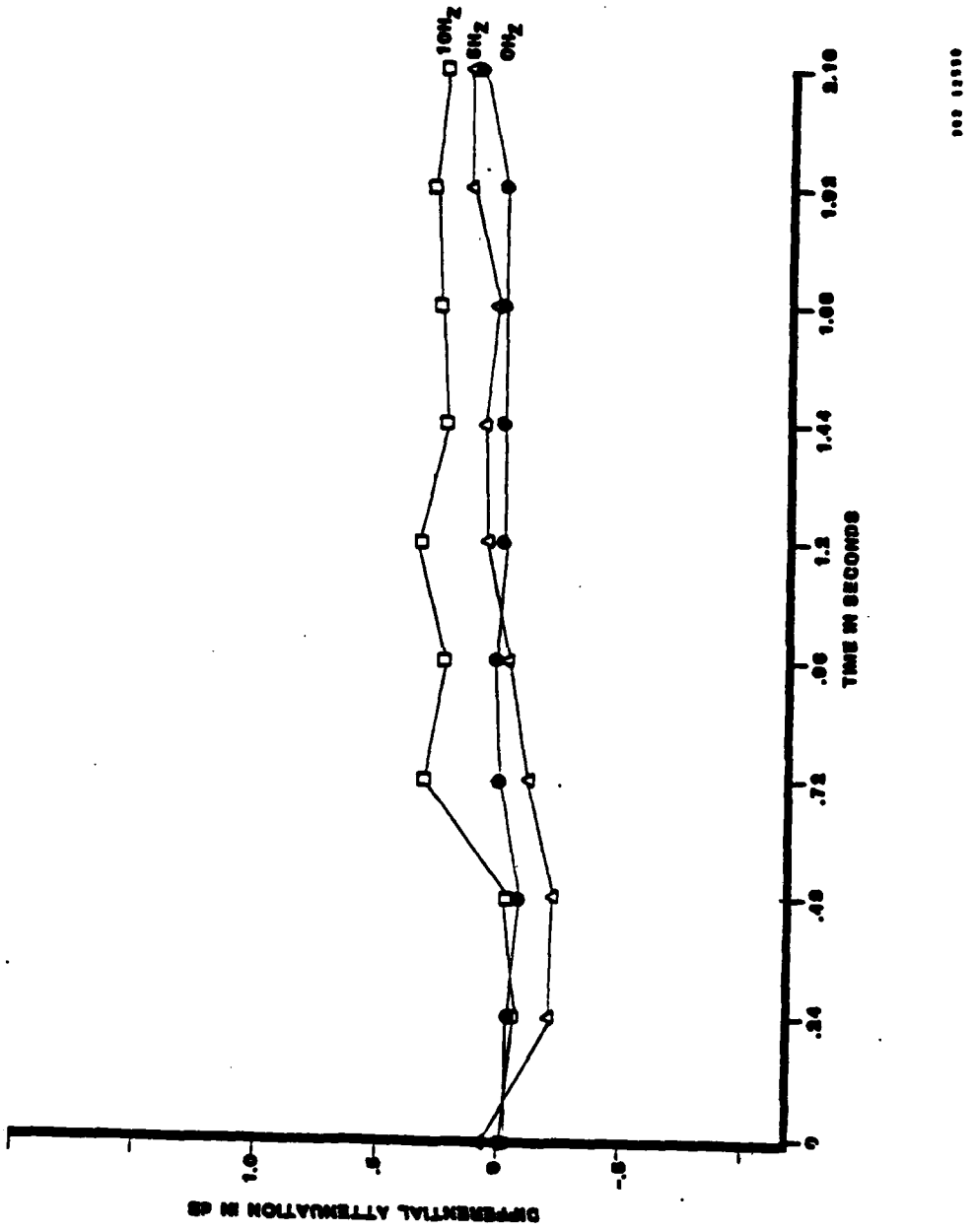

Figure 2.3.4-7.1. Bend Test 6.4 mm Mandrel EM-20495 Section 2.

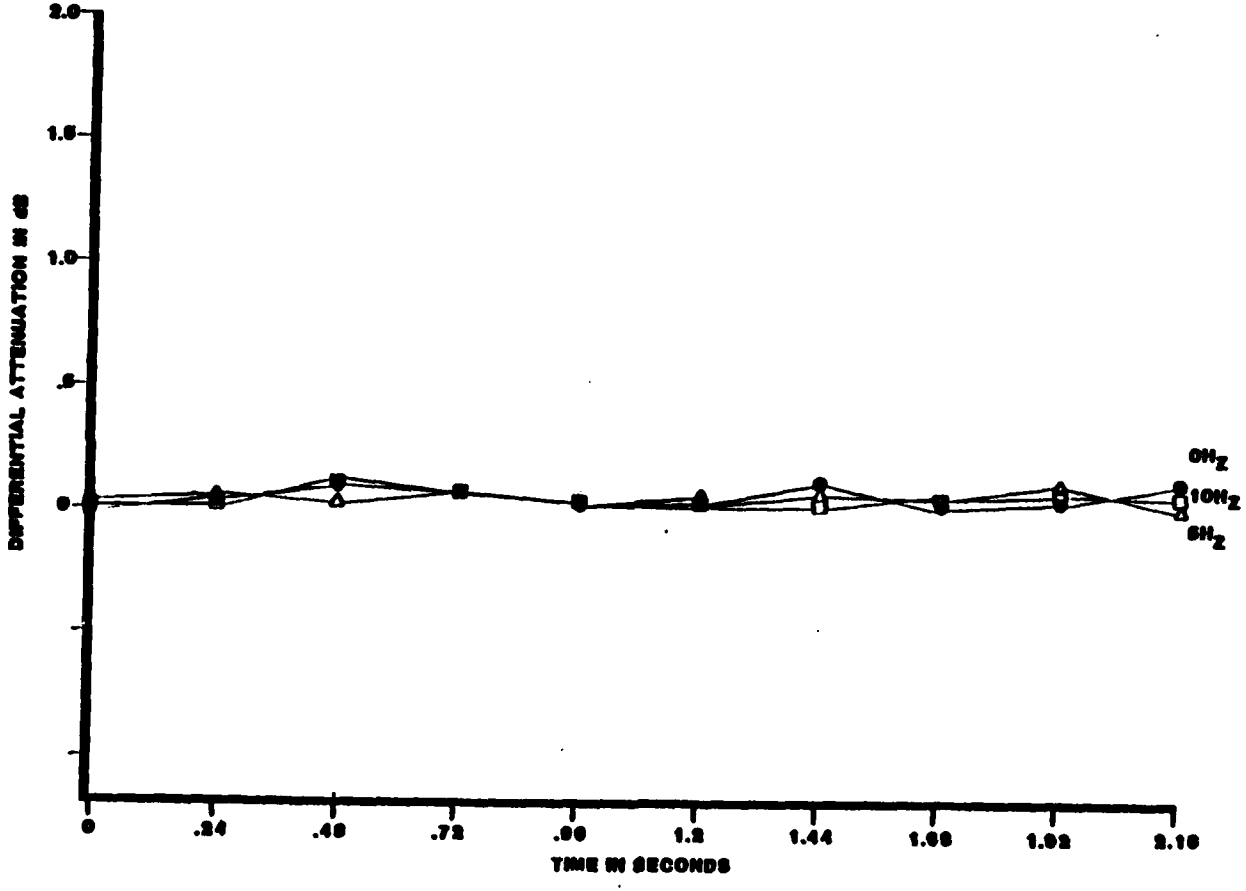

Figure 2.3.4-8.1. Bend Test 6.4 mm Mandrel EMH-20726c Section 1.

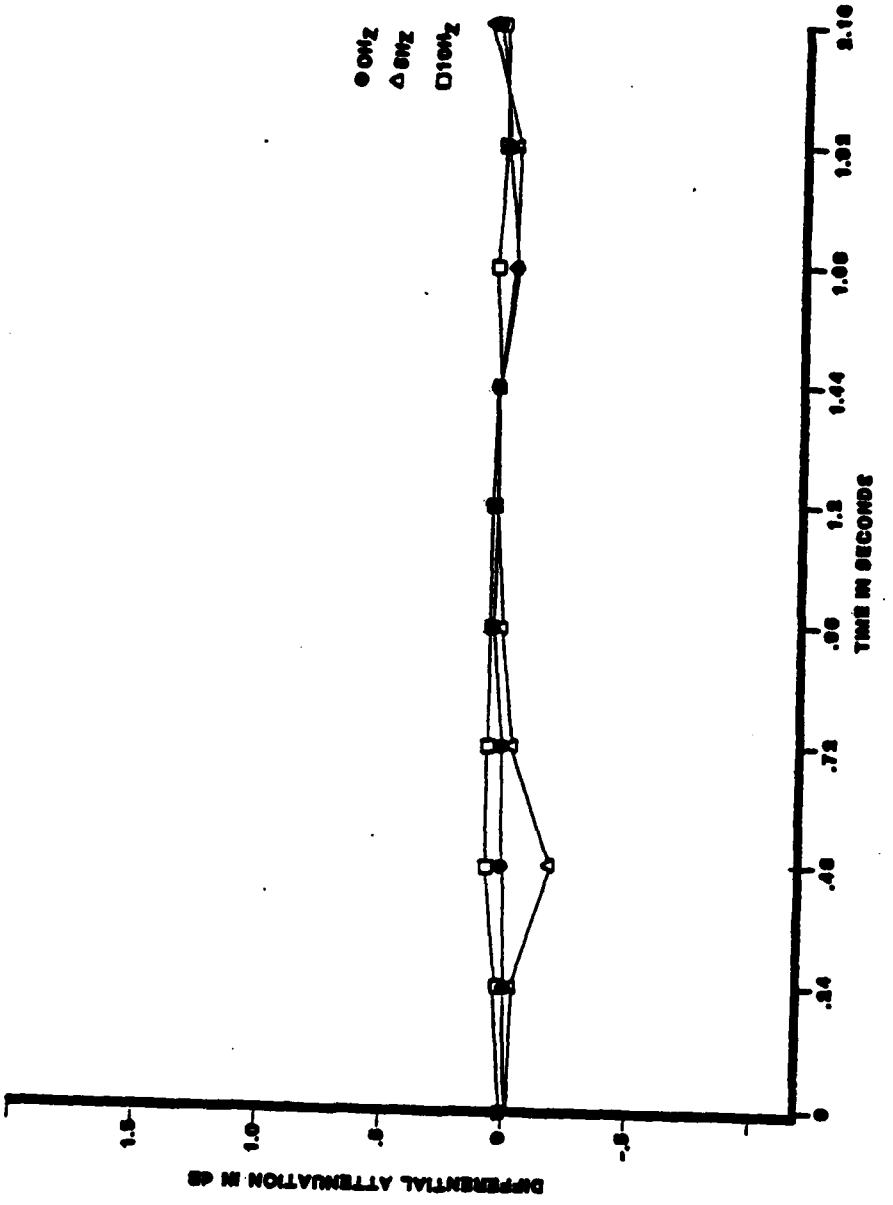

Figure 2.3.4-8.2. Bend Test 12.7 mm Mandrel EMH-20726c Section 1.

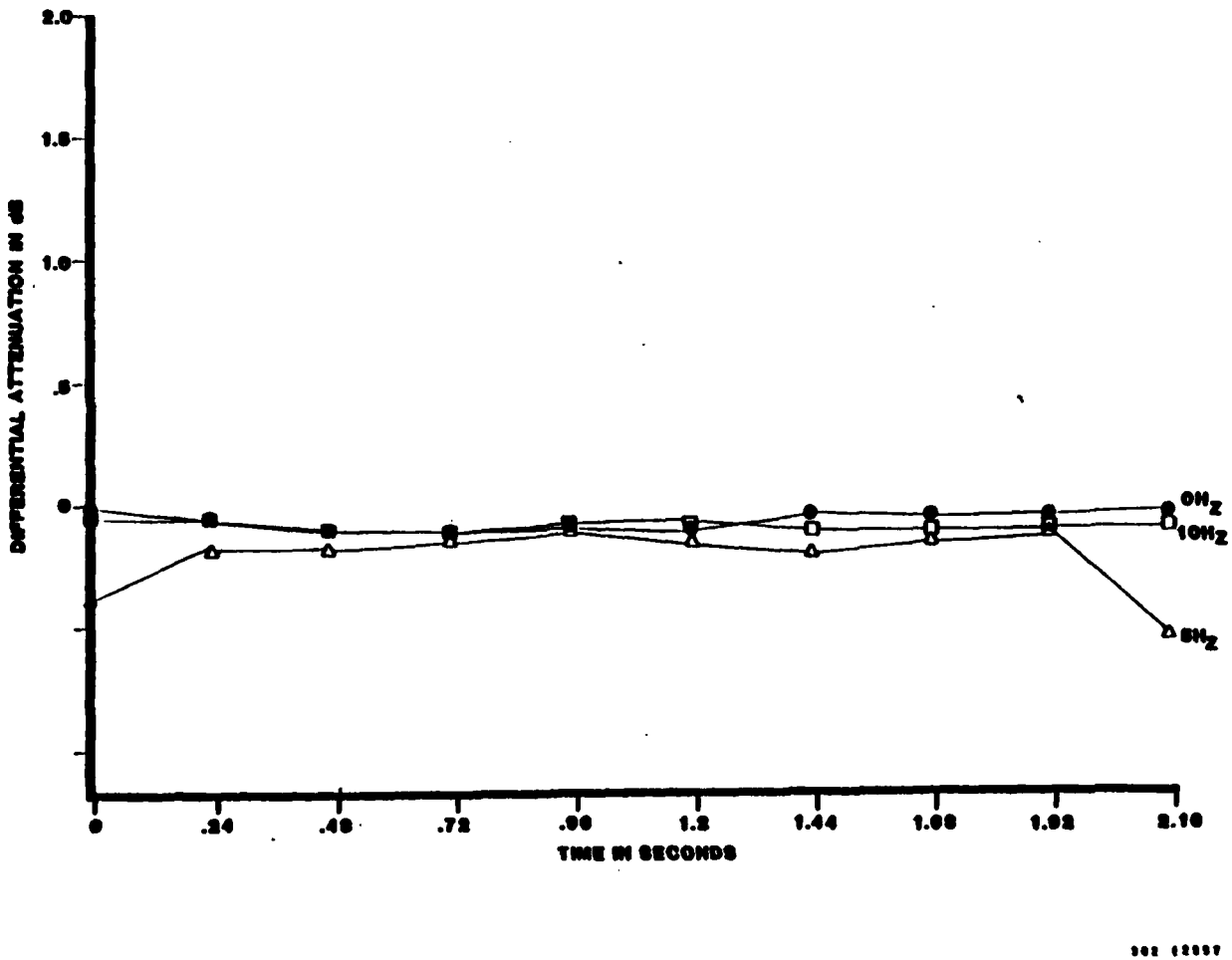

Figure 2.3.4-9.1. Bend Test 6.4 mm Mandrel EMH-20726c Section 2.

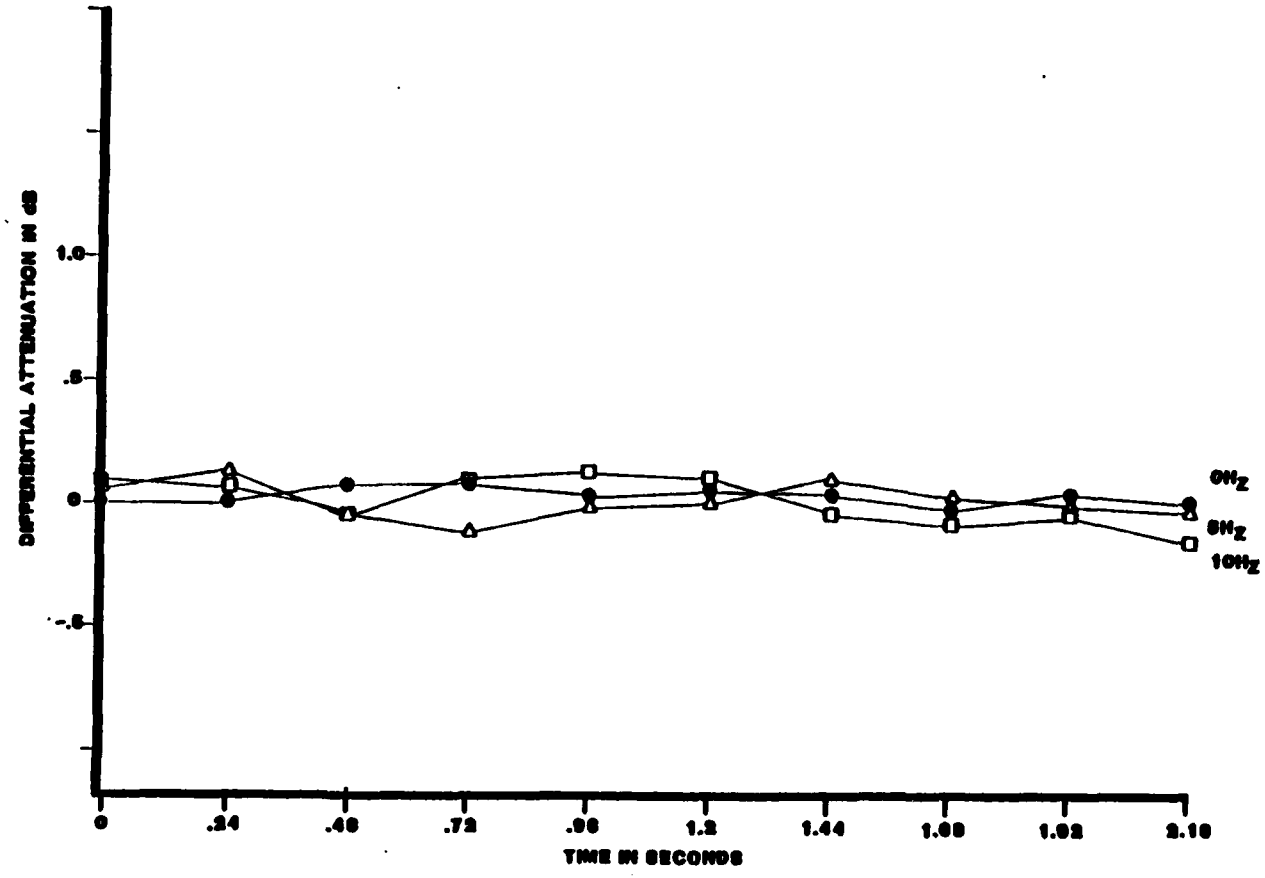

Figure 2.3.4-9.2. Bend Test 12.7 mm Mandrel EMH-20726c Section 2.

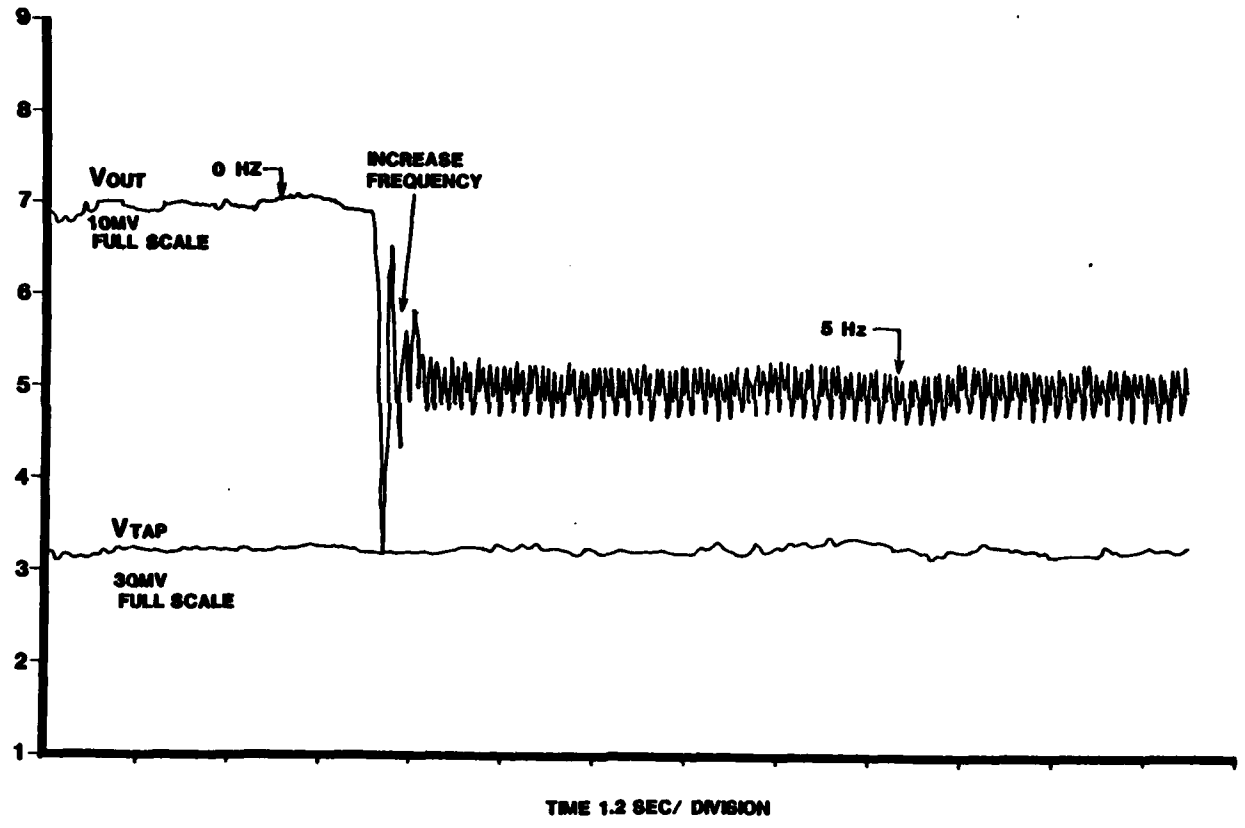

Figure 2.3.4-10. Sample Dynamic Bend Test Strip Chart.

However, as the sample strip chart of Figure 2.3.4-10 shows, a significant portion of the effect was filtered out by the lock in amplifier's bandwidth limitations. Therefore, the tests were repeated and the output waveforms photographed from a dual trace oscilloscope.

The photos obtained, shown in Figures 2.3.4-11 through 2.3.4-14, support the initial observations regarding mandrel diameters and fiber NA. Further, they show no dependence of induced attenuation on the stress frequency over the frequency range investigated.

The photos also show an imbalance in the bending stress applied to EMT-20793. This was due to a loose bolt during the test. The loose bolt allowed the mandrels to lift during one half of the cycle, reducing the stress. The maximum attenuations achieved are believed representative of the true condition.

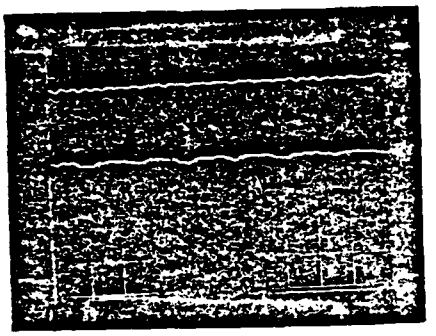

EMT-20721
Horizontal 50 ms/div
Vertical tap voltage, Upper Trace 20 mV/div
Output voltage, Lower Trace 20 mV/div

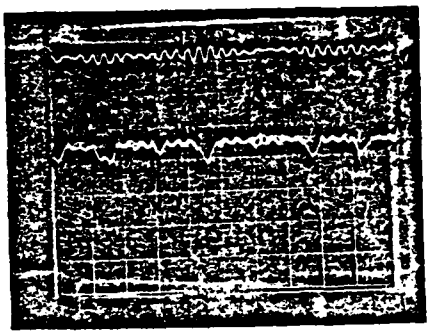

EMT-20793
Horizontal 50 ms/div
Vertical tap voltage, Upper Trace 5 mV/div
Output voltage, Lower Trace 10 mV/div

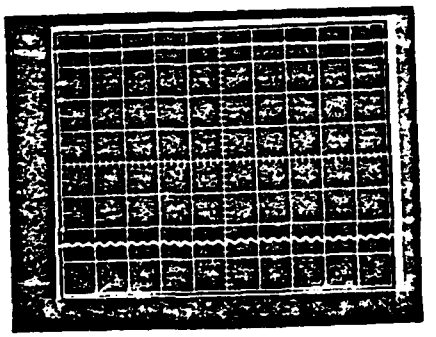

EM-20495
Horizontal 50 ms/div
Vertical tap voltage, Lower Trace 10 mV/div
Output voltage, Upper Trace 50 mV/div

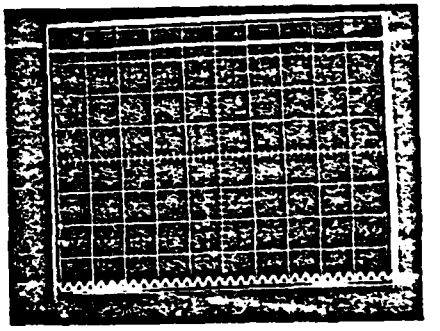

EMH-20726c
Horizontal 50 ms/div
Vertical tap voltage, Lower Trace 5 mV/div
Output voltage, Upper Trace 50 mV/div

Figure 2.3.4-11. 12.7 mm Mandrel Bend Test at 5 Hz.

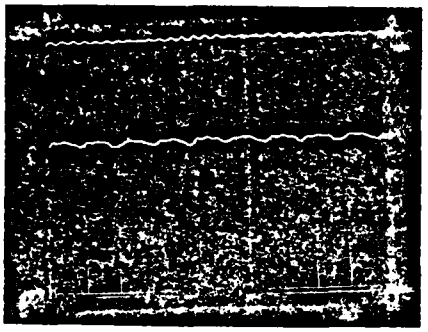

EMT-20721
Horizontal 50 ms/div
Vertical tap voltage, Upper Trace 20 mV/div
Output voltage, Lower Trace 20 mV/div

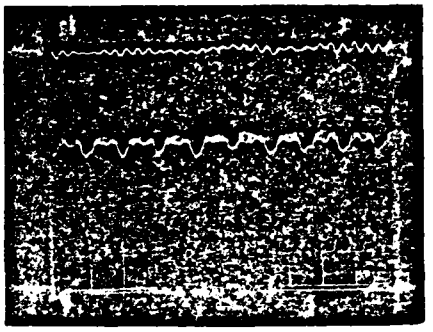

EMT-20793
Horizontal 50 ms/div
Vertical tap voltage, Upper Trace 5 mV/div
Output voltage, Lower Trace 10 mV/div

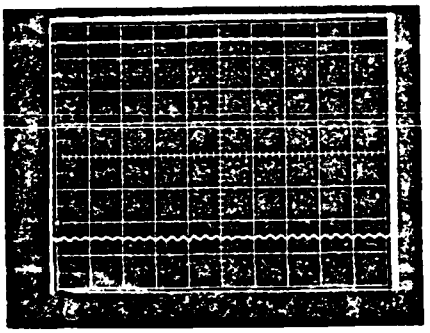

EM-20495
Horizontal 50 ms/div
Vertical tap voltage, Lower Trace 10 mV/div
Output voltage, Upper Trace 50 mV/div

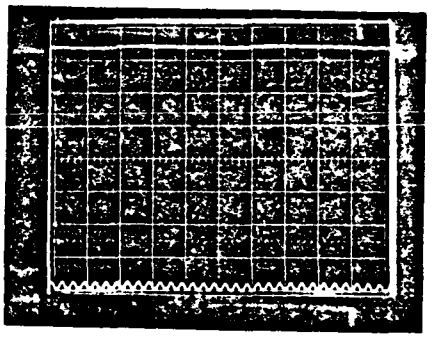

EMH-20726c
Horizontal 50 ms/div
Vertical tap voltage, Lower Trace 5 mV/div
Output voltage, Upper Trace 50 mV/div

Figure 2.3.4-12. 12.7 mm Mandrel Bend Test at 10 Hz.

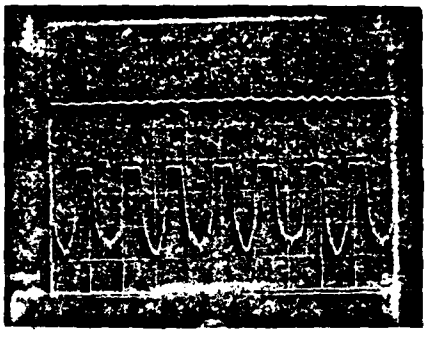

EMT-20721
Horizontal 50 ms/div
Vertical tap voltage, Upper Trace 20 mV/div
Output voltage, Lower Trace 20 mV/div

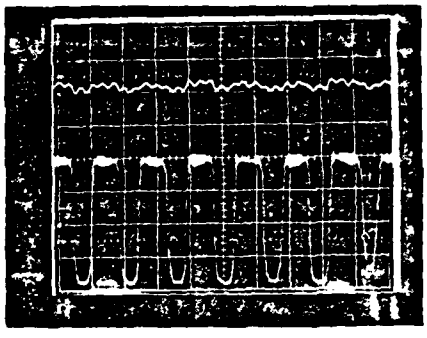

EMT-20793
Horizontal 50 ms/div
Vertical tap voltage, Upper Trace 5 mV/div
Output voltage, Lower Trace 10 mV/div

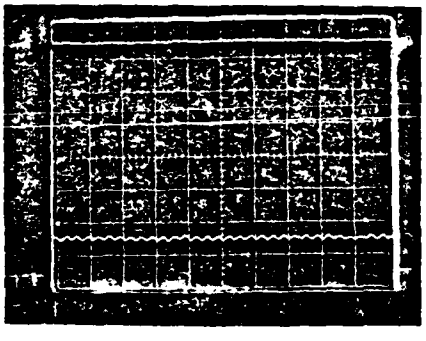

EM-20495
Horizontal 50 ms/div
Vertical tap voltage, Lower Trace 10 mV/div
Output voltage, Upper Trace 50 mV/div

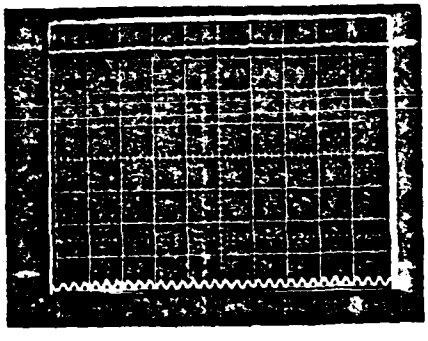

EMH-20726c
Horizontal 50 ms/div
Vertical tap voltage, Lower Trace 5 mV/div
Output voltage, Upper Trace 50 mV/div

Figure 2.3.4-13. 6.4 mm Mandrel Bend Test at 5 Hz.

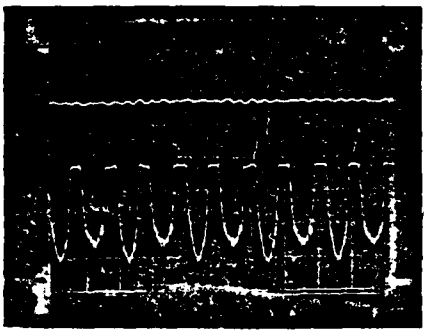

EMT-20721
Horizontal 50 ms/div
Vertical tap voltage, Upper Trace 20 mV/div
Output voltage, Lower Trace 20 mV/div

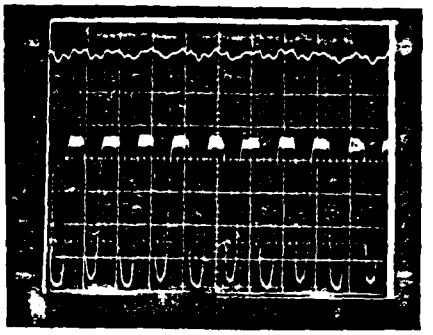

EMT-20793
Horizontal 50 ms/div
Vertical tap voltage, Upper Trace 5 mV/div
Output voltage, Lower Trace 10 mV/div

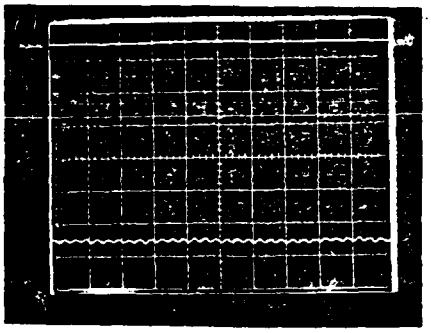

EM-20495
Horizontal 50 ms/div
Vertical tap voltage, Lower Trace 10 mV/div
Output voltage, Upper Trace 50 mV/div

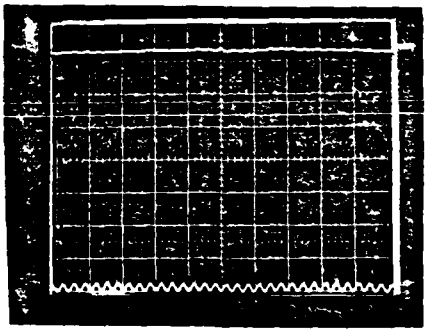

EMH-20726c
Horizontal 50 ms/div
Vertical tap voltage, Lower Trace 5 mV/div
Output voltage, Upper Trace 50 mV/div

Figure 2.3.4-14. 6.4 mm Mandrel Bend Test at 10 Hz.

3.0 CONCLUSIONS AND RECOMMENDATIONS

The experimental effort expended during this contract has established that the attenuation of both low and high NA single mode fibers is insensitive to either low frequency dynamic tension or dynamic twisting. Evaluation of fibers with respect to dynamic bending showed that low NA single mode fibers were attenuated during the bending phase while the high NA fibers were unaffected. Coating materials having refractive indices either higher or lower than fused quartz were applied to single mode fibers and were found to have no effect on dynamic attenuation characteristics. No effects arising from dynamic interactions were found in that all attenuation effects observed during dynamic testing were explained on the basis of static twists, tension, or bends.

Based on the results achieved and observations made during this contract, EOPD offers the following recommendations to further understand and improve the performance characteristics of single mode fibers designed for sensor applications:

a. Extend the dynamic effects evaluation of single mode fibers to acoustic levels. This study would increase the frequency of dynamic fiber perturbations to greater than 50 Hz.

b. Characterize single mode fiber bending loss with respect to numerical aperture over the NA range of 0.1 to 0.2 in order to establish optimal design trade offs between fiber handleability and core diameter.

c. Characterize single mode fiber bending loss with respect to variations in the V value from the cut-off at V_{CO} = 2.4 down to some fraction of V_{CO}. This would result in the definition of an effective operational wavelength range for fibers used in coiled or cabled configurations